Title

Reimagining dots and dashes: Visualizing structure and function of organelles for high-content imaging analysis

Journal

Cell Chemical Biology, 28(3)

ISSN

2451-9456

Authors

Chin, Marcus Y
Espinosa, Jether Amos
Pohan, Grace
et al.

Publication Date

2021-03-01

DOI

10.1016/j.chembiol.2021.01.016

Peer reviewed

HHS Public Access

Author manuscript

Cell Chem Biol. Author manuscript; available in PMC 2022 March 18.

Published in final edited form as:

Cell Chem Biol. 2021 March 18; 28(3): 320–337. doi:10.1016/j.chembiol.2021.01.016.

Reimagining dots and dashes: visualizing structure and function of organelles for high-content imaging analysis

Marcus Y. Chin[1], **Jether Amos Espinosa**[1], **Grace Pohan**[1], **Sarine Markossian**[1,2], **Michelle R. Arkin**[1,*]

[1]Small Molecule Discovery Center and Department of Pharmaceutical Chemistry, University of California, San Francisco, California 94143, USA

[2]Current Address: National Center for Advancing Translational Sciences, Rockville, Maryland 20892-4874 USA

SUMMARY

Organelles are responsible for biochemical and cellular processes that sustain life and their dysfunction causes diseases from cancer to neurodegeneration. While researchers are continuing to appreciate new roles of organelles in disease, the rapid development of specifically targeted fluorescent probes that report on the structure and function of organelles will be critical to accelerate drug discovery. Here, we highlight four organelles that collectively exemplify the progression of phenotypic discovery, starting with mitochondria, where many functional probes have been described, then continuing with lysosomes and Golgi and concluding with nascently described membraneless organelles. We introduce emerging probe designs to explore organelle-specific morphology and dynamics and highlight recent case studies using high content analysis in order to stimulate further development of novel probes and high-content approaches for organellar high throughput screening.

ELECTRONIC TABLE OF CONTENTS (eTOC)

Diseases from cancer to neurodegeneration induce changes in organellar structure and function. Innovative fluorescent probes allow live-cell monitoring of dynamic structural and functional changes by high-content analysis. Chin et al. highlights four organelles that exemplify phenotypic discovery from probe design to high-throughput screening for modulators of organelle function.

Graphical Abstract

*Correspondence and Lead Contact: michelle.arkin@ucsf.edu.

AUTHOR CONTRIBUTIONS

M.Y.C, J.A.E., G.P., S.M., and M.R.A. wrote and edited the manuscript.

DECLARATION OF INTERESTS

The authors declare no competing interests.

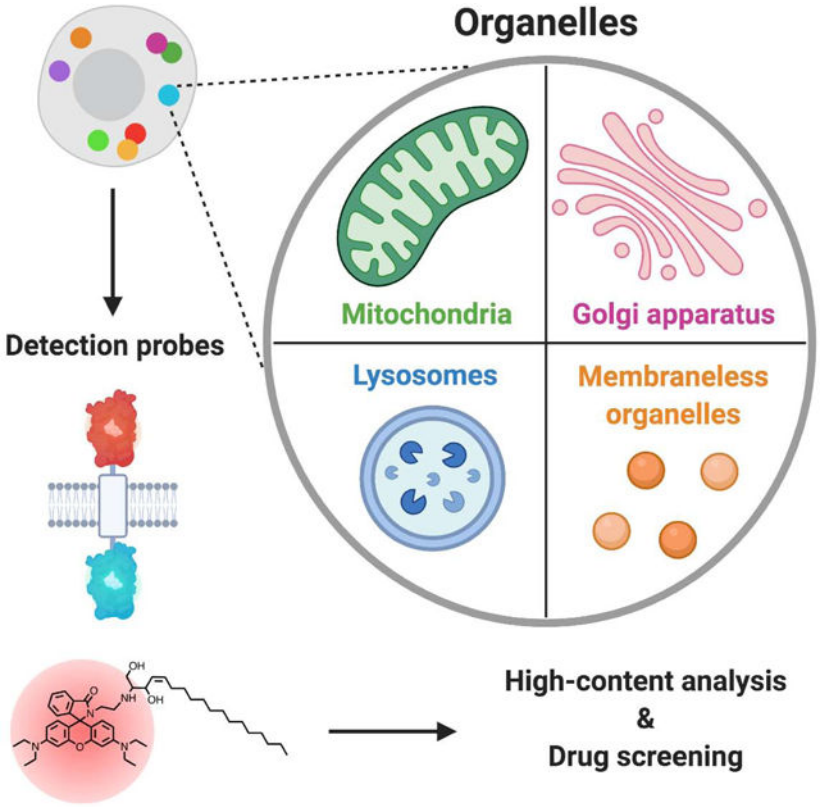

Keywords

Organelles; functional probes; high-content imaging; high-content analysis; drug screening; mitochondria; lysosome; Golgi apparatus; membraneless organelles

I. INTRODUCTION

Organelles are the main structural and functional subunits within our cells. They are the cellular factories and powerhouses involved in maintaining cell health and homeostasis. Disruption of specific organelle functions can be a cause or a symptom of cancer, neurodegeneration, and rare genetic diseases, among others. To discover compounds that correct these disruptions, phenotypic screens can take advantage of automated microscopy (high-content imaging or high-content analysis; HCA) and clinically relevant *in vitro* models such as those using patient-derived, induced pluripotent stem cells (iPSCs). Ideally, such sophisticated screens would include organelle-specific probes that report on the structure, function, and dynamics of organelles in live cells.

Fluorescent probes that target specific organelles include chemical dyes that bind based on particular biological features, such as net charge or lipophilicity, and genetically encoded protein sensors with fluorescent proteins (FPs) fused to an organelle-specific tag (Fig. 1A). Small-molecule probes tend to be bright and easy to use, while genetically encoded sensors have the advantages of high organellar specificity, controlled expression, low toxicity (for

extended live-cell imaging), and use in higher order models. Chemical and biological probes can be used to monitor *structural* features such as size, shape, number, and dynamics of the organelle. *Functional* probes also report on the organelle's biological function, such as the pH and protein degradation capacity of the lysosome or protein transport across the Golgi apparatus. HCA-based screens take advantage of structural and functional probes to discover and characterize molecules or genes that modulate organelle dysfunction. For HCA, ideal fluorophores have high photostability for live imaging, high quantum yield for sensitivity, and narrow excitation and emission spectra to allow multi-color imaging. Furthermore, fluorescence-based sensors should show low toxicity and minimally perturb organelle function.

For some organelles, an array of functional probes are already available; for others, organelle-specific sensors are being actively developed or sit on the more distant horizon (Rosania et al., 2003; Thompson et al., 2017; Valm et al., 2017; Zhu et al., 2016). For example, functional probes to quantify mitochondrial health have been utilized throughout the drug discovery industry, particularly to predict hepatotoxicity (Iannetti et al., 2019). For other organelles such as lysosomes, probes have largely concentrated on interrogating one functional aspect (e.g. pH) (Yue et al., 2016), but recent efforts aimed at improving probe specificity, encompassing other lysosomal functions into probe design and translating existing ones into screening paradigms. Functional probes for organelles such as the Golgi apparatus (herein known as the Golgi) and membraneless organelles (MLOs) are in development, and are just beginning to be utilized in high throughput applications.

Here, we introduce the state-of-the-art for the design and HCA application of organelle-specific sensors for these four organelles (Fig. 1B; Table S1). Additional organelles have been the subject of recent reviews (Daemen et al., 2015; Fam et al., 2018; Kempfer and Pombo, 2020; Lajoie et al., 2014; Panda et al., 2019; Weiss et al., 2018). The emergence of new probes will facilitate a better understanding of organellar biology and provide a platform to launch phenotypic screens with organelle-specific readouts that are directly correlated with diseases.

II. MITOCHONDRIA

Mitochondrial structure, function, and disease relevance

Mitochondria, often called "powerhouses" of the cell, produce adenosine triphosphate (ATP), the energy currency of most cellular processes. Mitochondria are composed of an outer and inner membrane, which is the site of ATP-generating oxidative phosphorylation. Highly convoluted cristae structures of the inner membrane increase surface area to maximize ATP yield through the electron transport chain (ETC). As electrons are shuttled through the ETC, the mitochondrial membrane potential ($\Delta\Psi$) forms between the negatively-charged matrix and positively-charged intermembrane space to maintain ATP production and storage (Fig. 2A). Additionally, mitochondria have important roles in regulating apoptosis, cellular redox homeostasis, intracellular calcium signaling, and neurogenesis (Ji et al., 2020; Khacho and Slack, 2018; Liu et al., 2020; Vringer and Tait, 2019). Interestingly, mitochondria are not synthesized *de novo*; instead, they are recycled through regulated cycles of fission and fusion (McInnes, 2013). Finally, mitochondria are the

only non-nuclei organelles in animal cells with their own DNA (mtDNA) that codes for RNAs and proteins involved in oxidative phosphorylation.

Mitochondrial dysregulation has broad implications in disease, particularly in neurodegeneration and myopathies. Neurons and muscle cells may be particularly vulnerable because their functions depend heavily on ATP consumption (Chanséaume and Morio, 2009; Mattson et al., 2008). Specific mutations in mitochondria-related proteins lead to myopathies such as Duchenne muscular dystrophy, where excessive calcium exposure leads to mitochondrial swelling, overproduction of reactive oxygen species (ROS), and increased mitochondrial permeability (Vila et al., 2017). Additionally, mitochondrial damage is also an effect of environmental toxins and drugs, particularly in the liver (drug-induced liver injury, or DILI) (Aleo et al., 2014). The diversity of mitochondrial dysfunctions in disease justifies the design of probes that monitor these different functions.

Structural and functional probes for mitochondria

The development of fluorescent dyes and genetically encoded probes to monitor mitochondrial function is advanced compared to many other organelles. Probes cover a broad array of mitochondrial features, including $\Delta\Psi$, mtDNA, ATP and ROS (Fig. 2A–D). Many of these are suitable for live imaging, allowing the measurement of dynamics. Furthermore, multiple probes have been used in combination to discover and characterize molecules that modulate mitochondrial function.

Cationic lipophilic dyes, such as tetramethylrhodamine methyl ester (TMRM) are functional probes that report on changes in $\Delta\Psi$. TMRM accumulates inside live mitochondria and forms temporary electrostatic interactions with the polarized $\Delta\Psi$ (Fig. 2A). When mitochondria are depolarized or damaged, these ionic interactions are lost, TMRM diffuses away, and mitochondrial fluorescence intensity decreases. TMRM also shows fast membrane equilibration, high specificity, low ETC inhibition, and low toxicity (Elmore et al., 2004). TMRM has been extensively used to investigate mitochondrial $\Delta\Psi$ in cancer cells; for instance, lung (A549, H446, SPC) and breast (MCF-7) cancer cells were shown to have higher $\Delta\Psi$ compared to noncancerous control cells (Creed and McKenzie, 2019; Zhang et al., 2015). More recent $\Delta\Psi$ probes like ECPI-12 (named after its modified C_{12}-alkyl chain) rely on hydrophobic interactions to localize to the inner mitochondrial membrane without permanently binding to thiol groups (Fig. 2A). Therefore, ECPI-12 is highly $\Delta\Psi$-independent and allows for high biocompatibility in situ and long-term tracking of mitochondria with fewer mitotoxic side-effects (Zhang et al., 2019) compared to commercially available dyes such as MitoTrackers that are reaction-based (Chazotte, 2011; Zhang et al., 2019).

Visualizing mtDNA provides another avenue to probe mitochondrial structure and function (Fig. 2B). Jevtic et al. tested whether a positively charged cyanine dye called SYBR Gold could selectively label mitochondrial nucleoids, the region within the mitochondria that houses mtDNA (Jevtic et al., 2018; Tuma et al., 1999). At low concentrations, SYBR Gold preferentially accumulated within unperturbed mitochondria in live cells. Super-resolution structured illumination microscopy (SIM) (Gustafsson et al., 2008) was then used to track mitochondrial nucleoid motion. Though at an early stage of development, mtDNA-binding

dyes like SYBR Gold could eventually probe mtDNA-related pathologies, such as systemic lupus erythematosus (Caielli et al., 2016), and be multiplexed with other functional dyes.

ATP levels are another important indicator of mitochondrial health. ATP is commonly measured by bioluminescent assays that detect the ATP-dependent luciferin-luciferase reaction (Crouch et al., 1993). These assays require cell lysis and are not selective for mitochondrial ATP; by contrast, an ideal ATP probe would work in living systems and bind specifically to mitochondrial ATP. To address these challenges, de la Fuente-Herreruela et al. introduced a small-molecule dye called rhodamine-based spirolactam (RSL^+) that accumulated specifically in mitochondria and measured mitochondrial ATP levels in live cells (de la Fuente-Herreruela et al., 2017) (Fig. 2C). Hydrogen bonding between the polyphosphates in ATP and the diethylenetriamine moiety in RSL^+ led to opening of the spirolactam ring, resulting in increased fluorescence. RSL^+ measured baseline ATP levels in human skin fibroblasts as well as ATP depletion in mouse embryonic fibroblasts treated with a mitochondrial toxin.

Adenosine 5-Triphosphate indicator based on epsilon (ε) subunit for analytical measurements (ATeam) is a genetically encoded ATP sensor based on fluorescence resonance energy transfer (FRET) (Fig. 2C). ATP binding causes a conformational change in the ε subunit of *Bacillus subtilis* F_0F_1-ATP synthase, bringing cyan-FP (CFP) and yellow-FP (YFP) variants in proximity to activate a FRET signal (Imamura et al., 2009). One *in vivo* study used ATeam to report mitochondrial ATP levels in a peripheral neuropathy mouse model. ATeam was fused to the mitochondrial targeting sequence of cytochrome c oxidase VIII (COX VIII) and was expressed in the demyelinated axons of mice (van Hameren et al., 2019). Van Hameren et al. concluded that in demyelinating neurodegenerative diseases, decreased mitochondrial ATP levels were due to dysregulated ATP production and increased export rate of mitochondrial ATP to the cytoplasm by ADP/ATP translocase. By localizing ATeam to the mitochondria, this study provided novel insight on the role that axonal mitochondria had on the production of ATP under pathological conditions.

Mitochondria are hotspots for the formation of ROS, which are important signaling molecules at normal concentrations; however, when mitochondria are damaged, electron leakage can result in the harmful overproduction of ROS (D'Autréaux and Toledano, 2007; Murphy et al., 2016). MitoSOX Red is a commonly used dye that discriminates between cellular and mitochondrial ROS production (De Biasi et al., 2016). MitoSOX Red targets the negatively charged mitochondrial inner membrane through the addition of the lipophilic, cationic substituent triphenyl phosphonium and fluoresces when it reacts with superoxide (Deshwal et al., 2018; Kaludercic et al., 2014) (Fig. 2D). Genetically encoded ROS sensors such as HyPer are based on yeast and bacterial ROS-detecting proteins and specifically measure hydrogen peroxide within mitochondria (Ermakova et al., 2014; Markvicheva et al., 2011).

There are several genetically encoded sensors that measure mitochondrial redox state (Liao et al., 2020). Fluorescent proteins roGFP1/2, rxYFP, and rxmRuby2 contain cysteine mutations near the proteins' chromophore (Banach-Latapy et al., 2014; Hanson et al., 2004; Piattoni et al., 2019). Under oxidative environments, the cysteine residues form a disulfide

bond and the chromophore is protonated, leading to a shift in its excitation spectrum (from 488 nm to 405 nm for roGFP, for instance). Relative redox environment is thus determined by exciting the protein at both wavelengths and measuring the fluorescence ratio. These probes can then be targeted to different regions within mitochondria by adding mitochondrial localization signal sequences. For instance, targeting rxYFP to the mitochondrial matrix and the intermembrane space demonstrated that the latter is more oxidizing than the former; furthermore, these probes showed that the redox properties of mitochondria and cytosol were independently regulated (Hu et al., 2008). Very recently, Werley et al. used the mitochondrial targeting sensor mito-roGFP2-Grx1 as part of an array of 20 genetically encoded sensors that have the potential to elucidate signaling cascades and mechanisms of action of chemical probes and drug leads (Werley et al., 2020).

Multiplexing mitochondrial probes for high-content analysis and screening

Mitochondrial dysfunction has become a focus for early diagnosis and intervention for neurodegenerative diseases (Peng et al., 2020). To study mitochondrial function in neurons, Varkuti et al. measured $\Delta\Psi$ and ATP levels, as reported by TMRM and luciferase respectively, in wild-type primary mouse neurons. Primary screening of 2,400 drugs identified 120 hits that promoted TMRM fluorescence and ATP generation, with a subset validated to promote mitochondrial respiration, mitochondria branching, and overall neurite area. Under neurodegenerative disease contexts such oxidative stress and Alzheimer's disease mutation, several drugs also protected against $\Delta\Psi$ decline (Varkuti et al., 2020). To develop a human-relevant screening model for Parkinson's disease (PD), Little et al. were the first to use HCA to evaluate mitochondria in iPSC-derived neurons from patients with mutations in α-synuclein, which is often mutated and aggregated in PD. In this assay, mitochondrial morphology and $\Delta\Psi$ were determined by measuring TMRM area and intensity, respectively. Cells were imaged and individually analyzed using automated confocal microscopy. PD patient-derived cells displayed reductions in $\Delta\Psi$ and altered mitochondrial area and length compared to healthy control neurons (Little et al., 2018).

Another study used amyotrophic lateral sclerosis (ALS) iPSC-derived motor neurons to screen for small-molecule regulators that increased axonal transport of mitochondria (Shlevkov et al., 2019) (Fig. 3A). In neurons, transport of mitochondria along the axon to distal dendritic networks is critical for neuronal function and communication; inhibition of axonal trafficking has been linked to disorders such as ALS (Magrané et al., 2014; Wang et al., 2013). Shlevkov et al. labeled mitochondria with the fluorescent protein Mito-DsRed, imaged every 2 seconds for 5 mins, and used an in-house analysis pipeline to quantify the percent of motile mitochondria and the average distance mitochondria traveled along axons and dendrites (Fig. 3B). From a screen of 3,200 molecules with known bioactivity, six compounds enhanced mitochondrial axonal transport in the ALS motor neurons. These compounds were reported to inhibit F-actin, Aurora Kinase B (AurKB) and Tripeptidyl peptidase 1 (TPP1); indeed, knocking down these genes phenocopied the effect of the small molecules. It is noteworthy that both the ALS and PD studies utilized patient-derived iPSCs differentiated into cell types relevant for the disease. Though using patient-derived cells increases the complexity of high-throughput screening, these systems may improve translation from assay to clinic.

Multiplexing of mitochondrial probes is widely used for studying drug-induced liver injury (DILI). DILI is a major cause of failure in drug development with mitotoxicity being one common cause of hepatotoxicity. Early testing for potential mitochondrial toxicity in high-throughput models could therefore significantly increase drug discovery success. Recently, Pohan et al. optimized a suite of high-throughput assays to measure mitochondria-related biomarkers indicative of DILI, including $\Delta\Psi$, ROS, and ATP, along with other cell health parameters including cell count, glutathione, and vacuolar density (Pohan et al., 2020). Although the assays utilized live cells, the multiplexed dyes were toxic to cells after prolonged exposure and were therefore incompatible for real-time cell monitoring. To enable live, kinetic monitoring of mitochondrial damage, Chandrasekharan et al. developed a screen based on the genetically encoded mt-roGFP2 to measure mitochondrial redox and TMRM to measure $\Delta\Psi$ (Chandrasekharan et al., 2019; Gutscher et al., 2008). Using time-lapse imaging, the authors demonstrated that mitochondrial oxidation preceded loss of membrane potential and mitochondrial permeability; this order of mitochondrial derangement was consistent for a library of anticancer agents. These studies demonstrate the utility of multiplexing small-molecule and genetically encoded probes for high-throughput and time-dependent measurement of mitochondrial damage for *in vitro* toxicology prediction.

The bidirectional relationship between mitochondrial ultrastructure and function, or morphofunction, is emerging as a crucial aspect of mitochondrial biology and disease (Bulthuis et al., 2019). Mitochondria morphofunction includes the dynamic fission and fusion of the mitochondrial outer and inner membranes, and the maintenance and regulation of cristae (Fig. 3C). These processes rapidly change given the physiological needs of the cell (Scott and Youle, 2010) and are dysregulated in multiple diseases (Archer, 2013; Koch et al., 2016; Waterham et al., 2007). For example, activating mutations in the protein-homeostasis regulator valosin-containing protein (VCP) lead to excessive degradation of mitofusin – a protein essential for mitochondrial fusion. VCP mutation thus leads to increased mitochondrial fission, decreased function, and myopathy (Zhang et al., 2017). Interestingly, small-molecule inhibitors of the mitochondrial outer membrane protein GTPase dynamin-related protein 1 may be able to reverse such excess fission (Bulthuis et al., 2019). In addition, morphofunction is phenotypically more complex than fission and fusion alone and requires sophisticated quantitative tools to explore mitochondrial phenotypic diversity. MitoGraph is an image analysis platform implemented by Harwig et al. to measure individual morphometric characteristics that range from entirely fragmented to hyper-elongated mitochondria (Harwig et al., 2018) (Fig. 3C). Mitochondria are detected through image segmentation and then classified through machine learning. MitoGraph has been validated to quantitatively analyze mitochondrial networks, volume, total length, and degree of branching in live and fixed cells. As another example, Iannetti et al. developed an unbiased HCA workflow to compare TMRM-stained mitochondria from two primary human skin fibroblast lines. Using confocal microscopy and multivariate analysis, over 30 mitochondrial descriptors were identified, including mitochondrial shape and branching (Iannetti et al., 2016). Morphofunction analysis could be a compelling approach for unbiased phenotypic drug screening for mitochondrial dysfunction.

Prospect of mitochondrial phenotypic discovery

Taking advantage of the unique structure, functions, and dynamics of mitochondria, diverse chemical and genetically encoded sensors have been developed. Many of these probes are active in live cells and have been incorporated into multiplexed screens and sophisticated cell models. While there is always room for innovation, the maturity of sensor development for mitochondria serves as inspiration for other organelles.

III. LYSOSOME

Lysosomal structure, function, and disease relevance

Lysosomes are small membrane-bound organelles that serve as major cellular sites for macromolecule degradation, a feat performed by lysosomal hydrolases that operate under acidic conditions. Enzymatic activity is ensured by tight regulation of lysosomal pH, which is profoundly acidic (pH~4.5) compared to other organellar compartments (Casey et al., 2010).

Low pH is set by the vacuolar-type H^+-ATPase (V-ATPase) pump that generates a proton gradient by hydrolyzing ATP. Other ion channels and transporters are also involved with balancing ion flux between the lysosomal lumen and cytosol (Mindell, 2012).

Lysosomes are part of the greater endolysosomal network that encompasses endocytosis, membrane trafficking, membrane maturation, and autophagy. This network is critical to cellular homeostasis and is implicated in many diseases. Compared to lysosomal assays, autophagy screening is relatively mature and has been previously reviewed (Fleming et al., 2011; Panda et al., 2019; Shu et al., 2012). In contrast to autophagy, endosomal probe development is more nascent. Defining endosomes is difficult due to the heterogeneous characteristics of endosomal types and biochemical markers (Naslavsky and Caplan, 2018). Lysosomes are positioned between autophagosomes and endosomes in terms of sensor and HCA development and represent an emerging target for phenotypic discovery.

For decades, lysosomes were regarded as static organelles that received and degraded waste. Relatively recently, they have garnered attention as potential primary therapeutic targets because of newly appreciated functions in protein homeostasis, cellular signaling, nutrient sensing, immune response, and secretion (Appelqvist et al., 2013; Settembre et al., 2013). In lysosomal storage disorders (LSDs), for instance, genetic mutations cause lysosomal enzyme deficiencies and impede the degradation of lipids and proteins. Accumulated waste material, such as cholesterol, is observed across different cell types, including those found in the central nervous system (Bi and Liao, 2010). Additionally, lysosomal enlargement is thought to cause lysosomal impairments, overall cellular dysfunction and cell death in LSDs. Likewise, underperforming lysosomes are linked to the pathogenesis of neurodegenerative diseases. For instance, lysosomal acidification defects are seen in Alzheimer’s disease models (Colacurcio and Nixon, 2016; Harguindey et al., 2007; Wolfe et al., 2013). The expression and activity of lysosomal enzymes such as cathepsins are also changed (Stoka et al., 2016). Together, these data suggest that abnormal lysosomal pH reduces degradative efficiency, compromising protein homeostasis and leading to neurodegenerative disease protein deposition. Cancers, by contrast, are characterized by hyperactive lysosomal

function, including alterations in lysosomal positioning, composition and volume. Increased activity of lysosomal hydrolases and their enhanced extracellular secretion degrades the extracellular matrix and allows cancer cells to become invasive (Kallunki et al., 2013; Kirkegaard and Jäättelä, 2009).

Lysosome-based screening

Because abnormal lysosomal function is strongly linked to disease pathogenesis, lysosome-specific probes are highly desirable for phenotypic screening. Several HTS studies have explored phenotypes such as lysosomal size, positioning, and calcium regulation in relation to LSDs and cancer (Fig. 4).

A majority of lysosome-based phenotypic screens have focused on LSDs. For example, to study Niemann-Pick disease type C (NPC), two independent groups developed HCA assays using patient-derived NPC fibroblasts to screen against lysosomal morphology and cholesterol accumulation (Fig. 4). NPC is caused by mutations in the cholesterol and lipid transporter genes *NPC1* or *NPC2*, which results in substrate buildup and enlargement of lysosomes. Xu et al. measured the fluorescence and size of lysosomes using LysoTracker, a dye that accumulates in acidic organelles. During assay validation, they found that methyl-β-cyclodextrin (MβCD), which is known to sequester cholesterol (Ilangumaran and Hoessli, 1998; Rosenbaum et al., 2010), reduced the size of enlarged lysosomes found in NPC cells (Xu et al., 2014). Pugach et al. further profiled lysosomal size with LysoTracker and immunofluorescence staining of lysosome-associated membrane protein 1 (LAMP1), a well-established marker of lysosomes. After screening 3532 drugs, kinase inhibitors, and metabolites, twenty-three compounds rescued NPC cholesterol accumulation, as stained by the cholesterol-binding dye fillipin. The antimicrobial compound alexidine was the most active and functioned by increasing mRNA transcript and protein levels of *NPC1* (Pugach et al., 2018).

Targeting lysosomal calcium release may also be a therapeutic approach for treating LSDs (Fig. 4). Disruption of calcium homeostasis is common to multiple LSDs and causes dysfunctional vesicle membrane dynamics and autophagy (Feng and Yang, 2016; Medina and Ballabio, 2015; Scotto Rosato et al., 2019). Colussi et al. developed a HTS assay to identify small molecules that restored lysosomal calcium function in Tay-Sachs disease (TSD) using patient-derived fibroblasts, which released lower levels of calcium from lysosome stores compared to wild-type cells (Colussi and Jacobson, 2019). Intracellular calcium was measured using a calcium-sensitive indicator Fluo-8 AM after induction of lysosomal calcium release. Primary screening of 1,200 FDA-approved drugs in TSD cells identified the antiparasitic drug pyrimethamine as the most active to restore wild-type levels of calcium release. Pyrimethamine, which accumulates in lysosomes (Clarke et al., 2011; Perrin, 1965), had been implicated in autophagy regulation (Giammarioli et al., 2012; Tommasino et al., 2016) and lysosomal activation (Jang et al., 2016).

Lysosomes traffic away from the perinuclear region towards the periphery during cancer growth and metastasis (Fig. 4). Tumorigenic stimuli such as acidic extracellular microenvironments promote anterograde lysosomal trafficking to the cell surface, where cathepsins are secreted to initiate tumor invasion (Steffan et al., 2009, 2011). To discover

therapeutics that inhibited this lysosomal movement, one study developed a HCA platform and identified modulators of lysosomal positioning in prostate cancer and glioma cells (Circu et al., 2016). Lysosomal positioning, as visualized by LAMP1, was determined based on the number of lysosomes that fell within a pre-designated ring region surrounding the nucleus compared to the cytosol and/or cell surface. From a screen of 2,210 FDA-approved drugs, eighteen compounds preferentially induced perinuclear lysosomal localization. Among the top hits was the antihelminthic drug niclosamide, which has previously been shown to affect cancer proliferation and survival pathways (Lee et al., 2020; Wang et al., 2018). Niclosamide inhibited cathepsin B secretion and blocked tumor cell migration in motility models. Interestingly, niclosamide altered lysosomal pH, suggesting a correlation between lysosomal acidity and positioning. Taken together, studies such as Pugach et al., Colussi et al., and Circu et al. exemplified the power of drug repurposing campaigns focused on screening lysosomal-specific phenotypes in disease-relevant cell models.

Functional probes targeted to lysosomes

Traditional lysosomal dyes are lipophilic, weak bases that pass through membranes and preferentially target acidic compartments such as lysosomes and late endosomes. Compared to their predecessors, newer generations of probes are organelle-selective and monitor lysosomal functions, providing advantages for future applications in HTS.

Both small-molecule and genetically encoded probes have been designed to measure lysosomal pH. Superior LysoProbes are rhodamine-based dyes that achieve specific lysosomal localization and probe retention by exploiting N-linked glycosylation, a common post-translational modification present on lysosomal membrane proteins that protects them from degradation (Chen et al., 2015) (Fig. 5A). Superior LysoProbes were conjugated with N-linked glycan moieties such as lactose and contained a fluorescent rhodamine spirolactam that was sensitive to acidic pH in the range of 4.8 to 6.0. The authors applied this probe to map both lysosomal position and pH changes in response to lobaplatin, a novel anticancer cisplatin analog that induced apoptosis. Compared to control, lobaplatin-treated cells showed enlarged and less acidic lysosomes that accumulated away from the perinuclear region. Thus, Superior LysoProbes were applied to profiling multiple derangements in lysosomes during apoptosis.

Very recently, three genetically encoded lysosomal pH probes have emerged, each focused on a different application. Each included the lysosomal protein LAMP1 fused to different fluorescent protein pairs to measure pH changes in the lysosomal lumen. One FP was selected for sensitivity to pH, while mCherry was used as a reference to normalize protein expression. Ponsford and colleagues created a probe called Ratiometric pHluorin (RpH)-LAMP1-3xFLAG, which detected pH from 4.0 to 7.0. The authors used this probe to map lysosomal pH in cell lines and primary neurons as a function of culture times and learned that pH was highly stable over several days in culture (Ponsford et al., 2020). Webb et al., designed pHLARE (pH Lysosomal Activity REporter), which used superfolder (sf) GFP to sense pH from 4.0 to 6.0 in cancer cells. Interestingly, transfecting the non-transformed breast cell line MCF10a with the oncogene hRASV12 lowered lysosomal pH from 5.23 to 4.67 (Webb et al., 2020). Finally, Chin and colleagues developed Fluorescence Indicator

Reporting pH of Lysosomes (FIRE-pHLy), using monomeric teal fluorescent protein 1 (mTFP1) as the pH sensor domain and measured pH from 3.5 to 6.0 (Fig. 5B) (Chin et al., 2020). FIRE-pHLy was stably expressed and demonstrated consistent response to the V-ATPase inhibitor bafilomycin in cancer cells, neurons, and in *Caenorhabditis elegans* animals. Notably, FIRE-pHLy quantitation used automated microscopy and analysis, demonstrating the potential for future HTS studies with this and potentially with related ratiometric pH sensors.

Besides pH, intraluminal chloride (Cl^-) concentration also plays a major role in lysosomal acidification by balancing the positive transmembrane voltage gradient generated by protons (Mindell, 2012). Deficits in chloride homeostasis lead to severe lysosomal pathologies. For example, deficiency of CLC-7, an H^+/Cl^- antiporter, causes both bone resorption failure and LSD-like neurodegenerative phenotypes (Kasper et al., 2005; Weinert et al., 2010). To better understand Cl^--mediated lysosomal dynamics, Leung et al. engineered a DNA-based ratiometric biosensor called ChloropHore, which simultaneously measured pH and Cl^- ions in lysosomes using two independent sensor domains based on small-molecule dyes previously described (Saha et al., 2015). An anionic integration domain aided in lysosomal targeting via receptor-mediated endocytosis (Fig. 5C). ChloropHore reported pH from 4.5 to 6.5 and physiological Cl^- concentrations from 5 mM to 120 mM (Chakraborty et al., 2017). Addition of ChloropHore to patient-isolated NPC fibroblasts identified differences in diseased lysosomal subpopulations. Compared to wild-type cells, NPC cells showed overall lower numbers of lysosomes with high Cl^- concentrations. Furthermore, the luminal Cl^- concentrations in perinuclear lysosomes was lower than in peripheral lysosomes, while pH was increased in both spatial types (Leung et al., 2019). These data indicated the pathological consequences of aberrant lysosomal distribution, pH, and chloride levels in NPC. This innovative study points the way to using dual ion measurements in future HTS campaigns.

Finally, Ishii et al. developed a genetically encoded protein trafficking probe, lysosomal MEasurement of protein Transporting integrity by RatIo Quantification (METRIQ), that is synthesized in the ER and traffics through the Golgi to lysosomes (Fig. 5D). The biosensor consists of a lysosomal resident protein (e.g. LAMP1) attached to sfGFP, a T2A self-cleaving peptide, and mCherry. Upon synthesis, lysosomal-METRIQ autocleaves and releases mCherry into the cytosol, providing an internal control for expression. The remaining lysosomal sfGFP fragment is shuttled into lysosomes where it is degraded and fluorescence is quenched. Therefore, changes in red/green fluorescence ratios indicate alterations in trafficking and lysosomal degradative function. 368 drugs known to inhibit intracellular signaling pathways were added to HeLa cells stably transfected with lysosomal-METRIQ and ratios were measured by flow cytometry. The cyclin-dependent kinase (CDK) inhibitors Kenpaullone and purvalanol A were among the top hits (Ishii et al., 2019). After target confirmation studies, CDK5 was determined to decrease lysosomal biogenesis independently of cell cycle arrest, although the exact mechanism remained to be elucidated. This study exemplified efforts to further elucidate new targets involved in lysosomal function by screening with lysosome-specific probes.

Prospect of lysosomal phenotypic discovery

Recent studies suggest a deeper complexity to lysosomal biology than previously imagined. Newer designs of probes bolster our understanding of lysosomes by providing more accurate labeling and functional measurements for pH, chloride, protease activity (Cheloha et al., 2019; To et al., 2015), and protein trafficking. Optimization of these functional sensors into HTS platforms will pave the way for discovery of compounds that normalize lysosomal functions altered in disease.

IV. GOLGI

Golgi structure, function, and disease relevance

The Golgi consists of interconnected stacks of flattened cisternae membranes that are responsible for packaging, processing and sorting molecular cargoes (lipids and proteins) to various cellular destinations. The Rab GTPases play master regulatory roles in cargo selection, transport, and membrane fusion events. Newly synthesized cargoes undergo anterograde trafficking from ER to the Golgi, where they are shuttled through the stacks, modified by enzymes, and exported. Golgi matrix and tethering proteins ensure proper structural integrity and movement through the Golgi, respectively. Retrograde Golgi-to-ER trafficking is also essential for retrieving ER export factors and Golgi soluble *N*-ethylmaleimide-sensitive factor attachment protein receptors (SNAREs) that allow for the fusion between membranes. The balance of inward and outward membrane trafficking maintains normal ER and Golgi functions. Stressors such as temperature, osmotic shock and drugs can disrupt this balance, causing the Golgi to collapse into the ER and resulting in cell death (Hicks and Machamer, 2005; Spang, 2013).

Golgi structure dynamically disassembles and reassembles during mitosis (Fig. 6A). Golgi dysregulation causes fragmentation or dispersal of the Golgi, a common disease phenomenon (Hicks and Machamer, 2005; Li et al., 2019). In neurodegenerative disorders, Golgi fragmentation is promoted by diverse molecular mechanisms. In early-stage AD, amyloid-beta peptides disrupt Golgi reassembly stacking proteins (Joshi et al., 2014, 2015). In PD, alpha-synuclein aggregation interferes with anterograde trafficking (Lashuel and Hirling, 2006). Finally in ALS, secretory vesicle trafficking is impaired (Atkin et al., 2014; Soo et al., 2015). Dysregulation of Golgi is also found in cancer, with mechanisms including aberrant glycosylation, overactivated Rab proteins, and elevated expression of Golgi-signaling kinases (Petrosyan, 2015). However, despite numerous examples of Golgi dysfunction, the relationship between Golgi morphofunction and disease remains unknown.

Phenotypic profiling of Golgi morphology using HCA methods

Since Golgi structure is complex and changes dynamically during healthy and disease states, the information captured by imaging Golgi is multidimensional. Image analysis has benefited from development of machine learning methods that allow images to be classified for different phenotypes even when these phenotypes have not been pre-defined (Fig. 6B, C). The use of machine learning in Golgi HCA provides an instructive example of how these methods can be used for multiple organellar phenotypes.

Three studies utilized supervised machine learning to automatically classify Golgi phenotypes in a high-throughput fashion (Fig. 6B) (Chia et al., 2012; Galea and Simpson, 2013; Galea et al., 2015). Galea et al. developed a supervised machine learning methodology using GFP fused to GalNAc-T, a Golgi resident protein, to classify normal and damaged Golgi phenotypes based on multiple features such as area and number of fragments. These authors then applied this approach to screen RNAi in a kinetic assay to uncover synergies between retrograde trafficking regulators (Galea et al., 2015). They stimulated retrograde transport with brefeldin A and measured GalNAc-T distribution between ER and Golgi at three time points to define retrograde transport rates. From this screen and further mechanistic experiments, the authors identified the critical roles of Rabs 1 and 6 in stimulating Golgi-ER trafficking.

Unsupervised machine learning may discover previously unrecognized Golgi fragmentation patterns (Fig. 6C). Hussain et al. explored a diversity of Golgi morphologies, as extracted from GalNAc-T staining and analyzed using an unsupervised clustering framework (Hussain et al., 2017). From this model, new Golgi phenotypes were described and protein-protein interactions were predicted based on related phenotypic signatures. For example, the SNARE proteins STX18, GOSR2, USE1, USO1, and STX5 were predicted to associate based on phenotypic similarity; these proteins had previously been shown to affect ER and Golgi trafficking (Dilcher et al., 2003; Shorter et al., 2002; Xu et al., 2000), and were predicted to form physical complexes (Hussain et al., 2017). Thus, unsupervised clustering models described many additional Golgi phenotypes that were useful for uncovering new biological associations.

Golgi probes with improved targeting and functionality

Small molecule probes targeting Golgi typically contain fluorophores conjugated to sphingolipids that concentrate in the Golgi during trafficking and metabolism. For example, 7-nitrobenz-2-oxa-1,3-diazole (NBD)-ceramide and BODIPY-ceramide dyes are used for imaging Golgi in live cells. However, because ceramide analogs can localize to other compartments of the cell, more specific Golgi-targeted probes are needed. Recent probes have focused on improving Golgi-targeting while others use a combination of targeting and biosensor groups to simultaneously measure Golgi function.

L-cysteine provides a novel Golgi targeting mechanism inspired by the cysteine-dependent anchoring of abundant Golgi resident proteins (Aoki et al., 1992; Maeda et al., 2001). Aoki et al. first demonstrated that cysteine residues within the membrane-anchoring domain of galactosyltransferase are required for Golgi retention. Similarly, Maeda et al. reported that protein kinase D, a key regulator of Golgi vesicle dynamics, is also recruited to the Golgi network via its cysteine-rich domain. Applying this concept, Li and colleagues designed an L-cysteine carbon quantum dot (LC-CQD) nanoprobe that targeted Golgi (Fig. 5E). LC-CQDs significantly improved Golgi localization compared to D-cysteine-CQDs, indicating that cysteine chirality strongly influenced targeting capability. Other advantages of the probe included high brightness and excellent photostability. Cells incubated with LC-CQD could be imaged continuously for one hour, which was six times longer than the fluorescence of

BODIPY-ceramide or genetically encoded N-acetylgalactosaminyltransferase-GFP (Li et al., 2017).

Functional probes have been developed to measure Golgi luminal pH. Fan et al. developed a small molecule probe that monitored changes in Golgi acidification in both live cells and *in vivo* settings. The fluorescence probe, termed RSG, was composed of Golgi-targeting sphingosine conjugated to pH-sensitive rhodamine spirolactam (Fig. 5F) (Fan et al., 2019). Another Golgi pH sensor was synthesized by Deschamps et al. The genetically encoded probe was composed of a fusion between pHluorin, a pH-sensitive GFP-based sensor, and Mnn2, a Golgi membrane-associated enzyme (Fig. 5G). Golgi pH varies along the stack to govern normal protein glycosylation (Kellokumpu et al., 2002), changing from pH 6.7 near the ER (*cis*) to 6.0 near the plasma membrane (*trans*) (Paroutis et al., 2004). The pHluorin probe was used to map *cis*- and *medial*-Golgi pH and to differentiate the roles of yeast V-ATPase subunits (Deschamps et al., 2020). Since defects in Golgi pH are linked to cancer and cystic fibrosis, among other diseases (Rivinoja et al., 2012), screening for compounds that modulate Golgi pH could yield important chemical probes and new drug targets.

One group developed an iron-sensitive probe with the goal of elucidating the emerging role of Golgi in iron metabolism. Iron homeostasis is crucial for controlling oxidative damage of labile, or unbound, Fe(II) in the cell. Furthermore, missorting of the iron transporter DMT1 is linked to neurodegenerative diseases (Belaidi and Bush, 2016). Using their previously developed Fe(II)-specific chemical switch, Hirayama and colleagues synthesized Gol-SiRhoNox to measure labile Fe(II) Golgi pools. Gol-SiRhoNox consisted of a myristoyl motif to aid in Golgi targeting and a silicon-fused rhodamine modified with *N*-oxide that fluoresced after Fe(II)-mediated cleavage (Fig. 5H) (Ishida et al., 2013). Gol-SiRhoNox measured Fe(II) distribution in protein-sorting deficient systems. While Fe(II) distribution was normally Golgi dominant, deletion of the protein-sorting machinery shifted Fe(II) and DMT1 localization to lysosomes. However, rescue by a molecular chaperone led to redistribution of DMT1 and Fe(II) to the Golgi (Hirayama et al., 2019).

Anterograde trafficking from ER to Golgi can be challenging to study because anterograde and retrograde transport occur in tandem. Boncompain and colleagues have built an innovative system called Retention Using Selective Hook (RUSH) to synchronize transport of a protein cargo by controlling its release from a donor compartment, e.g., ER (Boncompain et al., 2012). The RUSH system uses two fusion proteins. One fusion protein includes streptavidin attached to a signal sequence “hook” that localizes streptavidin to the donor compartment; the second fusion protein contains cargo fused to a fluorescent protein and a streptavidin-binding peptide (SBP). The fluorescent cargo is held in the donor compartment by SBP binding to streptavidin. When biotin is added to cells, SBP is released and the cargo traffics normally to the acceptor compartment, thus allowing imaging of uni-directional protein trafficking. The RUSH assay was adapted to screen for small-molecule regulators of anterograde trafficking in HeLa cells (Boncompain et al., 2019). In this screen, ManII, a Golgi glycosylase, was tagged with eGFP and SBP; streptavidin was fused with the ER-retention signal peptide KDEL as the hook. Upon treatment with biotin, ManII was released and transported to the Golgi acceptor compartment within thirty minutes. From a library of 640 FDA-approved drugs, two epithelial growth factor receptor (EGFR) inhibitors,

BML-265 and Tyrphostin AG1478, caused cargo to remain in the ER; these effects were reversible when the compound was removed. Both compounds also inhibited anterograde trafficking of EGFR to prevent its localization on the cell surface, which has clinical implications in cancer (Tomas et al., 2014).

Prospect of Golgi phenotypic discovery

Golgi phenotypic discovery is being accelerated by powerful HCA techniques, which allow visualization of the complex relationship between Golgi structure, dynamics, and trafficking. Additionally, innovative probes that achieve better Golgi specificity and the ability to sense pH and Fe(II) provide ripe opportunities for phenotypic screening.

V. MEMBRANELESS ORGANELLES

Membraneless organelles (MLOs) structure, function, and disease relevance

Membraneless organelles (MLOs) are non-membrane-bound subcellular compartments that perform specialized biochemical functions (Crabtree and Nott, 2018) (Fig. 7A, B). MLOs exist in both the nucleus and cytoplasm as liquid foci caused by liquid-liquid phase separation (LLPS) of specific RNAs and proteins (Alberti et al., 2019; Boeynaems et al., 2018; Chong et al., 2018; Weber and Brangwynne, 2012). MLOs play various roles in RNA processing, ribonucleoprotein (RNP) assembly, and cellular stress response (Anderson and Kedersha, 2002; Chang et al., 2018; Fan and Leung, 2016; Galganski et al., 2017; Kimball et al., 2003; Lafarga et al., 2016; Lallemand-Breitenbach and de Thé, 2010; Luo et al., 2018; Morris, 2008; Pederson, 2011; Spector and Lamond, 2011; Tripathi et al., 2012; Waris et al., 2014). They are also highly dynamic structures; in many cases, proteins and RNAs exchange with MLOs on the seconds-minutes time scale, allowing these bodies to respond quickly to changes in cell state (Chang et al., 2018; Moon et al., 2019). A summary of the different MLOs, their functions, constituents, and detection probes can be found in Table S2. Interest in MLOs for chemical biology and drug discovery has dramatically increased in the past five years, and methodologies for visualizing MLOs were recently reviewed (Mitrea et al., 2018). Due to their small size (~0.1 – 5 μm) and highly dynamic nature, these structures are the vanguard for design of functional HCA probes and high-throughput phenotypic screens.

Given the important roles of MLOs in cellular homeostasis, perturbations in organellar constituents could affect their function and dynamics, leading to progression of diseases such as ALS and cancer. For instance, promyelocytic leukemia nuclear bodies (PML-NBs) contain around 30 proteins, including tumor suppressors (p53, PML), DNA repair factors, and apoptotic inducers. PML-NBs are often down-regulated in cancer, suggesting a resistance to DNA damage-mediated cell death and apoptosis (Chang et al., 2018; Guan and Kao, 2015; Gurrieri et al., 2004; Lallemand-Breitenbach and de Thé, 2010; Reineke and Kao, 2009). Stress granules (SGs) are another MLO that form in the presence of a wide array of cellular stresses, and contain translationally stalled mRNA and stalled 48S preinitiation complexes (Anderson and Kedersha, 2002; Fan and Leung, 2016; Kimball et al., 2003; Waris et al., 2014). In ALS, patient cells have been found to contain mutant fused in sarcoma (FUS) and/or mutant TAR-DNA binding protein of 43 kDa (TDP-43) in SGs. This recruitment may impact cellular defense mechanisms and lead to disease progression

(Baron et al., 2013; Wolozin and Ivanov, 2019). Mutations of FUS and TDP-43 occur in low-complexity domains, protein regions with a low diversity of amino acid composition, perhaps leaving them more vulnerable to self-association and phase-separation (Conicella et al., 2016; Elbaum-Garfinkle, 2019; Murakami et al., 2015).

MLO-based screening

Two of the drivers for HCA technology development for MLOs are their associations with disease pathology and their novel properties compared to membrane-bound organelles. Due to their small size and complex dynamics, MLOs require careful image analysis protocols (Caragine et al., 2019; He et al., 2018; Major et al., 2017). Here, we highlight a few imaging-based screening studies that either show relevance of MLOs in chemical biology/drug discovery or employ advanced imaging techniques. These screens use structural probes, including fluorescence *in situ* hybridization (FISH) to identify RNAs (Jain et al., 2016; Wang et al., 2019), and immunofluorescence or FP fusions to monitor proteins in MLOs (Marrone et al., 2018; Platani et al., 2000). Of these three methods, only genetically encoded fusion proteins are amenable to live-cell screening.

Yip et al. developed a phenotypic screening assay to identify compounds that induced PML-NBs formation as an anticancer strategy (Yip et al., 2011). They noted that the beneficial effects of interferon (INF) and arsenical (As_2O_3) treatments in cancer are due to PML-NB formation, but their high toxicities dampen their effectiveness as anticancer treatments. The authors hypothesize that compounds inducing PML-NB formation directly would restore the tumor suppressor activity of PML with lower toxicity. For the screen, PML-NBs were visualized by immunofluorescence staining of PML protein in fixed HeLa cells and were identified as stained puncta within the nucleus. A library of 1280 drugs and a pooled combinatorial library containing millions of compounds were screened, using IFN-gamma as a positive control. Additionally, since DNA-damaging agents upregulate PML-NBs, markers for direct DNA damage (phosphorylated H2AX histone and phosphorylated Chk1 kinase) were included as counter screens. The high-content screen of the combinatorial library identified N-methyl triamine-containing compounds that induced PML-NB formation without causing phosphorylation of H2AX and Chk1. This early example of an HCA screen for MLOs also demonstrated the feasibility of counting these small objects in high throughput.

As noted above, the recruitment of FUS to SGs is associated with impaired stress responses in ALS. Disease-causing mutations such as P525L in the nuclear localization signal (NLS) of FUS are particularly prone to SG recruitment (Marrone et al., 2018). To discover drugs and mechanisms to reduce FUS localization to SGs, Marrone et al. developed HCA assays in iPSCs and iPSC-derived motor neurons using fusion proteins containing eGFP fused to wild-type (wt) or P525L-FUS. These FUS-eGFP fusions were added via CRISPR/Cas9 gene-editing, leading to near-wild-type expression levels. Under stress, SGs containing P525L-FUS-eGFP appeared larger and brighter than granules containing wtFUS-eGFP, indicating an impairment in SG dynamics. Screening 1600 existing drugs in P525L-FUS-eGFP cells identified several autophagy inducers, including rapamycin and known CNS-active drugs, that minimized size, number, and intensity of mutant SGs. Interestingly, the

authors showed that fewer than 5% of SGs co-stained for the autophagy marker LC3, suggesting that FUS-eGFP itself, rather than FUS-eGFP-containing SGs, were degraded by autophagy. This conclusion was in agreement with one published study (Ganassi et al., 2016), and in contrast to another one that found colocalization of autophagosomes and FUS + SGs (Ryu et al., 2014). In addition to the biological insight provided by this screen, several technical features are noteworthy. This manuscript appears to be the first to report an HCA screen measuring endogenous SGs in live iPSCs and motor neurons. Also, adding fluorescent fusions into the endogenous locus of the protein-of-interest via gene editing allowed wild-type regulation and expression. This study thus represents a significant advancement towards the goal of measuring membraneless organelle function and dynamics in human-relevant cell models.

Nuclear speckles are among the most complex MLOs; they are involved in mRNA processing and contain hundreds of proteins and RNAs. Remarkably, Fei et al. demonstrated sub-organellar spatial organization (Fei et al., 2017) within the nuclear speckle using single-molecule FISH (smFISH) and immunofluorescence, coupled with superresolution microscopy (SIM) (Fig. 7C). Furthermore, Wang et al. used FISH technology to develop an imaging-based pooled-CRISPR screening methodology to identify proteins that modulated localization of long noncoding RNA (lncRNA) to nuclear speckles (Wang et al., 2019). They used lentiviral transfection to co-deliver bar-coded single guide RNAs (sgRNAs) targeting potential regulatory RNA-binding proteins and a FISH-based reporter for the lncRNA of interest. They then performed single-cell, multiplex error-robust FISH (MERFISH) to read the barcodes of the corresponding sgRNA that induced or inhibited recruitment of the lncRNA into the nuclear speckles. To demonstrate the potential of this technology, they screened 162 sgRNAs targeting 54 RNA binding proteins and successfully identified known positive and negative regulators of the lncRNA MALAT1. Two of these RNA-binding proteins, heterogeneous nuclear (hn)RNPH1 and hnRNPK, were also shown to affect localization of other nuclear speckle constituents such as U2 small nuclear (sn)RNA, poly-A-containing RNAs, preribosomal RNA, and MRP, suggesting that perturbations of hnRNP genes could lead to abnormal nuclear speckle formation.

Interestingly, a few studies have shown that different MLOs work together in processing RNAs and RNPs. For example, assembled snRNPs are transported from Cajal bodies to nuclear speckles for protein modification, and mRNAs are transported from SGs to processing bodies (p-bodies) for degradation (Fan and Leung, 2016; Morris, 2008). Other linkages between MLOs are yet to be discovered. Using pools of siRNAs targeting 1354 human genes, Berchtold et al. developed a multiplexed HCA platform to immunostain six different MLOs and identified genes regulating MLO formation, as well as shared regulatory pathways (Berchtold et al., 2018). For example, down-regulation of cAMP phosphodiesterases increased the number of p-bodies, while cAMP-dependent protein kinase (PKA) was required for formation of Cajal bodies. Furthermore, genes regulating nucleolar morphology were also found to be involved in splicing-related functions of nuclear speckles. This finding was in agreement with previous studies where follicular cells with a mutation in a splicing factor gene SRRM2 exhibited smaller nucleoli (Policarpio-Nicolas and Sirohi, 2013; Tomsic et al., 2015). Thus, MLOs are not only highly dynamic organelles, but also form a complex network for RNA and protein processing in the cell.

Development of MLO-targeted probes

Fluorescent probe development for MLOs is rapidly expanding. Small-molecule fluorophores and RNA sensors for live-cell applications will offer advantages and complementarity to current methods for high-content and high-throughput applications.

To our knowledge, chemical probes targeting MLOs have so far only been demonstrated for ribosomal (r)DNA and rRNA detection (Fig. 7D). Several reported dyes, however, suffer from poor photostability, selectivity, and/or cell permeability (Li et al., 2006, 2013; Song et al., 2014). A thiazole orange (TO)-based dye with a styryl substituent creates a highly selective probe called styryl-TO that intercalates into the G-quadruplex structures of rDNA in live PC3 cells (Lu et al., 2015, 2016). The probe exhibits high rDNA-to-dsDNA selectivity due to its styryl moiety. The deep red fluorescence probe CP and a naphthalimide dye called probe 1 are also demonstrated to have good rRNA-to-DNA selectivity, photostability, and compatibility with live-cell imaging (Cao et al., 2019; Liu et al., 2015; Zhou et al., 2015). Both CP and probe 1 bind to rRNA through hydrophobic interactions. CP has been used to monitor live nucleoli dynamics prior, during, and after mitosis in HeLa cells (Zhou et al., 2015). As reported by other studies (Dundr et al., 2000; Leung et al., 2004), nucleoli were found distorted and reduced in size, finally disappearing during mitosis and reassembling during telophase. This study exemplified the potential of small-molecule probes to monitor MLO dynamics.

Advanced RNA-detection methodologies, largely focused on single-molecule detection, have generated deep insight into RNA dynamics in MLOs and provide an exciting opportunity for live-cell HCA for screening applications. These probes were very recently reviewed (Braselmann et al., 2020). Briefly, approaches include fluorescent-protein fusions with RNA-binding proteins, molecular beacons, and dye-binding RNA-based aptamers. Aptamers are nucleic acid sequences that are selected for binding to particular targets. Since Jaffrey and co-workers described aptamers that bind to small-molecule dyes (Filonov et al., 2014; Paige et al., 2011), several groups have developed genetically-encoded RNA sensors that bind to cell-permeable dyes in live cells (Cawte et al., 2020; Yatsuzuka et al., 2018). As a recent example, Cawte et al. used a FRET-based aptamer fused to a reporter mRNA to demonstrate detection of single mRNA molecules in MLOs called paraspeckles.

Prospects for MLOs phenotypic discovery

MLO-based screens have focused on structure and composition. Emerging small-molecule and RNA-based probes could enable high-throughput screening platforms in live cells to visualize dynamic readouts such as rates of organelle fusion, trafficking, and colocalization of RNAs and proteins on a much larger scale. Both the biology and technology to study MLOs are rapidly co-evolving.

OUTLOOK

Phenotypic screening has become increasingly prevalent as a means to identify active small molecules in human-relevant disease models. However, after primary screening, determining a compound’s mechanism of action often becomes a major obstacle; approaches that

accelerate this process are needed. Looking forward, organellar-based phenotypic discovery may fill this gap by incorporating higher specificity of mechanistic information, while maintaining clinically-relevant cellular phenotypes in assay design. Exciting new developments are on the horizon with the emergence of improved chemical and genetically encoded probes for organelles. Effective designs target probes to specific organelles - and even suborganellar compartments - while measuring organelle-specific functions. By combining newer generations of functional probes with powerful HCA and patient-derived cells, future HTS studies have the capacity to generate large amounts of disease-relevant multi-parametric data that can be explored to identify not only new molecular targets but also therapeutic leads for drug discovery.

SIGNIFICANCE

Organelles are defined cellular compartments, each with its own unique structure and function. Past technologies were tremendously useful in elucidating these properties; however, as our understanding of organellar functions and dynamics deepens, so will the need to develop more specific tools. As exemplified in this review, organelles are not static structures – mitochondria undergo fusion and fission, lysosomes traffic to and from the nucleus, Golgi disperses and reforms during mitosis and stress, and MLO constituents assemble rapidly in response to different cellular states. Specific probes are enabling accurate labeling of organelles and even suborganellar structures, and will allow for multiplexed measurements of organelle systems. Recently, there has been an emphasis on organelle-specific screens using primary and patient-derived cells that recapitulate the cellular contexts of disease, promising better translation from the bench to clinic. Taken together, organellar phenotypic discovery is brimming with novel probes and technologies that are only just being applied to HTS platforms. In this review, we introduced several key organelles where we see active and innovative phenotypic discovery with emphasis on tool development and HTS case studies.

Supplementary Material

Refer to Web version on PubMed Central for supplementary material.

ACKNOWLEDGEMENTS

We would like to thank Dr. Yanzhuang Wang and his laboratory (University of Michigan) for providing immunofluorescence images for Figure 6A. This work was supported by R01 AG057342 (M.C., M.R.A.) and the University of California National Laboratories, Office of the President and GlaxoSmithKline (J.A.E., G.P., S.M., M.R.A.).

REFERENCES

Alberti S, Gladfelter A, and Mittag T. (2019). Considerations and challenges in studying liquid-liquid phase separation and biomolecular condensates. Cell 176, 419–434. [PubMed: 30682370]

Aleo MD, Luo Y, Swiss R, Bonin PD, Potter DM, and Will Y. (2014). Human drug-induced liver injury severity is highly associated with dual inhibition of liver mitochondrial function and bile salt export pump: ALEO ET ALet al. Hepatology 60, 1015–1022. [PubMed: 24799086]

Anderson P, and Kedersha N. (2002). Stressful initiations. J Cell Sci 115, 3227–3234. [PubMed: 12140254]

Aoki D, Lee N, Yamaguchi N, Dubois C, and Fukuda MN (1992). Golgi retention of a trans-Golgi membrane protein, galactosyltransferase, requires cysteine and histidine residues within the membrane-anchoring domain. PNAS 89, 4319–4323. [PubMed: 1584766]

Appelqvist H, Wäster P, Kågedal K, and Öllinger K. (2013). The lysosome: from waste bag to potential therapeutic target. Journal of Molecular Cell Biology 5, 214–226. [PubMed: 23918283]

Archer SL (2013). Mitochondrial Dynamics — Mitochondrial Fission and Fusion in Human Diseases. N Engl J Med 369, 2236–2251. [PubMed: 24304053]

Atkin JD, Farg MA, Soo KY, Walker AK, Halloran M, Turner BJ, Nagley P, and Horne MK (2014). Mutant SOD1 inhibits ER-Golgi transport in amyotrophic lateral sclerosis. J. Neurochem. 129, 190–204. [PubMed: 24134191]

Banach-Latapy A, He T, Dardalhon M, Vernis L, Chanet R, and Huang M-E (2014). P37 - Monitoring dynamic changes of glutathione redox state in subcellular compartments of human cells – an approach based on rxYFP biosensor. Free Radical Biology and Medicine 75, S33.

Baron DM, Kaushansky LJ, Ward CL, Sama RRK, Chian R-J, Boggio KJ, Quaresma AJC, Nickerson JA, and Bosco DA (2013). Amyotrophic lateral sclerosis-linked FUS/TLS alters stress granule assembly and dynamics. Molecular Neurodegeneration 8, 30. [PubMed: 24090136]

Belaidi AA, and Bush AI (2016). Iron neurochemistry in Alzheimer's disease and Parkinson's disease: targets for therapeutics. Journal of Neurochemistry 139, 179–197.

Berchtold D, Battich N, and Pelkmans L. (2018). A Systems-Level Study Reveals Regulators of Membrane-less Organelles in Human Cells. Molecular Cell 72, 1035–1049.e5.

Bi X, and Liao G. (2010). Cholesterol in Niemann–Pick Type C disease. Subcell Biochem 51, 319–335. [PubMed: 20213549]

Boeynaems S, Alberti S, Fawzi NL, Mittag T, Polymenidou M, Rousseau F, Schymkowitz J, Shorter J, Wolozin B, Van Den Bosch L, et al. (2018). Protein Phase Separation: A New Phase in Cell Biology. Trends Cell Biol 28, 420–435. [PubMed: 29602697]

Boncompain G, Divoux S, Gareil N, de Forges H, Lescure A, Latreche L, Mercanti V, Jollivet F, Raposo G, and Perez F. (2012). Synchronization of secretory protein traffic in populations of cells. Nat Methods 9, 493–498. [PubMed: 22406856]

Boncompain G, Gareil N, Tessier S, Lescure A, Jones TR, Kepp O, Kroemer G, Del Nery E, and Perez F. (2019). BML-265 and Tyrphostin AG1478 Disperse the Golgi Apparatus and Abolish Protein Transport in Human Cells. Front Cell Dev Biol 7.

Braselmann E, Rathbun C, Richards EM, and Palmer AE (2020). Illuminating RNA Biology: Tools for Imaging RNA in Live Mammalian Cells. Cell Chemical Biology 27, 891–903. [PubMed: 32640188]

Bulthuis EP, Adjobo-Hermans MJW, Willems PHGM, and Koopman WJH (2019). Mitochondrial Morphofunction in Mammalian Cells. Antioxidants & Redox Signaling 30, 2066–2109. [PubMed: 30266077]

Caielli S, Athale S, Domic B, Murat E, Chandra M, Banchereau R, Baisch J, Phelps K, Clayton S, Gong M, et al. (2016). Oxidized mitochondrial nucleoids released by neutrophils drive type I interferon production in human lupus. Journal of Experimental Medicine 213, 697–713.

Cao C, Wei P, Li R, Zhong Y, Li X, Xue F, Shi Y, and Yi T. (2019). Ribosomal RNA-Selective Light-Up Fluorescent Probe for Rapidly Imaging the Nucleolus in Live Cells. ACS Sens 4, 1409–1416. [PubMed: 31017390]

Caragine CM, Haley SC, and Zidovska A. (2019). Nucleolar dynamics and interactions with nucleoplasm in living cells. ELife 8, e47533.

Casey JR, Grinstein S, and Orlowski J. (2010). Sensors and regulators of intracellular pH. Nat Rev Mol Cell Biol 11, 50–61. [PubMed: 19997129]

Cawte AD, Unrau PJ, and Rueda DS (2020). Live cell imaging of single RNA molecules with fluorogenic Mango II arrays. Nature Communications 11, 1283.

Chakraborty K, Leung K, and Krishnan Y. (2017). High lumenal chloride in the lysosome is critical for lysosome function. ELife 6, e28862.

Chandrasekharan A, Varadarajan SN, Lekshmi A, Lupitha SS, Darvin P, Chandrasekhar L, Pillai PR, Santhoshkumar TR, and Pillai MR (2019). A high-throughput real-time in vitro assay using

mitochondrial targeted roGFP for screening of drugs targeting mitochondria. Redox Biology 20, 379–389. [PubMed: 30408753]

Chang HR, Munkhjargal A, Kim M-J, Park SY, Jung E, Ryu J-H, Yang Y, Lim J-S, and Kim Y. (2018). The functional roles of PML nuclear bodies in genome maintenance. Mutation Research/Fundamental and Molecular Mechanisms of Mutagenesis 809, 99–107. [PubMed: 28521962]

Chanséaume E, and Morio B. (2009). Potential Mechanisms of Muscle Mitochondrial Dysfunction in Aging and Obesity and Cellular Consequences. Int J Mol Sci 10, 306–324. [PubMed: 19333447]

Chazotte B. (2011). Labeling Mitochondria with MitoTracker Dyes. Cold Spring Harbor Protocols 2011, pdb.prot5648-pdb.prot5648.

Cheloha RW, Li Z, Bousbaine D, Woodham AW, Perrin P, Volarić J, and Ploegh HL (2019). Internalization of Influenza Virus and Cell Surface Proteins Monitored by Site-Specific Conjugation of Protease-Sensitive Probes. ACS Chem. Biol. 14, 1836–1844. [PubMed: 31348637]

Chen X, Bi Y, Wang T, Li P, Yan X, Hou S, Bammert CE, Ju J, Gibson KM, Pavan WJ, et al. (2015). Lysosomal Targeting with Stable and Sensitive Fluorescent Probes (Superior LysoProbes): Applications for Lysosome Labeling and Tracking during Apoptosis. Sci Rep 5, 9004. [PubMed: 25758662]

Chia J, Goh G, Racine V, Ng S, Kumar P, and Bard F. (2012). RNAi screening reveals a large signaling network controlling the Golgi apparatus in human cells. Molecular Systems Biology 8, 629. [PubMed: 23212246]

Chin MY, Patwardhan AR, Ang KK, Wang AL, Alquezar C, Welch M, Arkin MR, and Kao AW (11 2020). Genetically encoded ratiometric biosensor for probing lysosomal pH in mammalian cells and C. elegans. (BioRxiv pre-print). doi: 10.1101/2020.11.04.368654.

Chong S, Dugast-Darzacq C, Liu Z, Dong P, Dailey GM, Cattoglio C, Heckert A, Banala S, Lavis L, Darzacq X, et al. (2018). Imaging dynamic and selective low-complexity domain interactions that control gene transcription. Science 361.

Circu ML, Dykes SS, Carroll J, Kelly K, Galiano F, Greer A, Cardelli J, and El-Osta H. (2016). A Novel High Content Imaging-Based Screen Identifies the Anti-Helminthic Niclosamide as an Inhibitor of Lysosome Anterograde Trafficking and Prostate Cancer Cell Invasion. PLoS ONE 11, e0146931.

Clarke JTR, Mahuran DJ, Sathe S, Kolodny EH, Rigat BA, Raiman JA, and Tropak MB (2011). An open-label Phase I/II clinical trial of pyrimethamine for the treatment of patients affected with chronic GM2 gangliosidosis (Tay–Sachs or Sandhoff variants). Mol Genet Metab 102, 6–12. [PubMed: 20926324]

Cohen S, Valm AM, & Lippincott-Schwartz J. (2018). Interacting organelles. Current Opinion in Cell Biology, 53, 84–91. 10.1016/j.ceb.2018.06.003 [PubMed: 30006038]

Colacurcio DJ, and Nixon RA (2016). Disorders of lysosomal acidification—The emerging role of v-ATPase in aging and neurodegenerative disease. Ageing Research Reviews 32, 75–88. [PubMed: 27197071]

Colussi DJ, and Jacobson MA (2019). Patient-Derived Phenotypic High-Throughput Assay to Identify Small Molecules Restoring Lysosomal Function in Tay–Sachs Disease. SLAS DISCOVERY: Advancing the Science of Drug Discovery 24, 295–303.

Conicella AE, Zerze GH, Mittal J, and Fawzi NL (2016). ALS mutations disrupt phase separation mediated by -helical structure in the TDP-43 low complexity C-terminal domain. Structure 24, 1537–1549. [PubMed: 27545621]

Crabtree M, and Nott T. (2018). These Organelles Have No Membranes.

Creed S, and McKenzie M. (2019). Measurement of Mitochondrial Membrane Potential with the Fluorescent Dye Tetramethylrhodamine Methyl Ester (TMRM). In Cancer Metabolism: Methods and Protocols, Haznadar M, ed. (New York, NY: Springer), pp. 69–76.

Crouch SPM, Kozlowski R, Slater KJ, and Fletcher J. (1993). The use of ATP bioluminescence as a measure of cell proliferation and cytotoxicity. Journal of Immunological Methods 160, 81–88. [PubMed: 7680699]

Daemen S, van Zandvoort MAMJ, Parekh SH, and Hesselink MKC (2015). Microscopy tools for the investigation of intracellular lipid storage and dynamics. Mol Metab 5, 153–163. [PubMed: 26977387]

D'Autréaux B, and Toledano MB (2007). ROS as signalling molecules: mechanisms that generate specificity in ROS homeostasis. Nature Reviews Molecular Cell Biology 8, 813–824. [PubMed: 17848967]

De Biasi S, Gibellini L, Bianchini E, Nasi M, Pinti M, Salvioli S, and Cossarizza A. (2016). Quantification of mitochondrial reactive oxygen species in living cells by using multi-laser polychromatic flow cytometry: Quantification of Mitochondrial Reactive Oxygen Species. Cytometry 89, 1106–1110. [PubMed: 27575554]

Deschamps A, Colinet A-S, Zimmermannova O, Sychrova H, and Morsomme P. (2020). A new pH sensor localized in the Golgi apparatus of Saccharomyces cerevisiae reveals unexpected roles of Vph1p and Stv1p isoforms. Sci Rep 10, 1881. [PubMed: 32024908]

Deshwal S, Antonucci S, Kaludercic N, and Di Lisa F. (2018). Measurement of Mitochondrial ROS Formation. In Mitochondrial Bioenergetics, Palmeira CM, and Moreno AJ, eds. (New York, NY: Springer New York), pp. 403–418.

Dilcher M, Veith B, Chidambaram S, Hartmann E, Schmitt HD, and Fischer von Mollard G. (2003). Use1p is a yeast SNARE protein required for retrograde traffic to the ER. EMBO J 22, 3664–3674. [PubMed: 12853481]

Dundr M, Misteli T, and Olson MOJ (2000). The Dynamics of Postmitotic Reassembly of the Nucleolus. J Cell Biol 150, 433–446. [PubMed: 10931858]

Elbaum-Garfinkle S. (2019). Matter over mind: Liquid phase separation and neurodegeneration. J Biol Chem 294, 7160–7168. [PubMed: 30914480]

Elmore SP, Nishimura Y, Qian T, Herman B, and Lemasters JJ (2004). Discrimination of depolarized from polarized mitochondria by confocal fluorescence resonance energy transfer. Archives of Biochemistry and Biophysics 422, 145–152. [PubMed: 14759601]

Ermakova YG, Bilan DS, Matlashov ME, Mishina NM, Markvicheva KN, Subach OM, Subach FV, Bogeski I, Hoth M, Enikolopov G, et al. (2014). Red fluorescent genetically encoded indicator for intracellular hydrogen peroxide. Nature Communications 5, 5222.

Fam TK, Klymchenko AS, and Collot M. (2018). Recent Advances in Fluorescent Probes for Lipid Droplets. Materials (Basel) 11.

Fan AC, and Leung AKL (2016). RNA Granules and Diseases — A Case Study of Stress Granules in ALS and FTLD. Adv Exp Med Biol 907, 263–296. [PubMed: 27256390]

Fan L, Wang X, Ge J, Li F, Zhang C, Lin B, Shuang S, and Dong C. (2019). A Golgi-targeted off–on fluorescent probe for real-time monitoring of pH changes *in vivo*. Chem. Commun. 55, 6685–6688.

Fei J, Jadaliha M, Harmon TS, Li ITS, Hua B, Hao Q, Holehouse AS, Reyer M, Sun Q, Freier SM, et al. (2017). Quantitative analysis of multilayer organization of proteins and RNA in nuclear speckles at super resolution. J Cell Sci 130, 4180–4192. [PubMed: 29133588]

Feng X, and Yang J. (2016). Lysosomal Calcium in Neurodegeneration. Messenger (Los Angel) 5, 56–66.

Filonov GS, Moon JD, Svensen N, and Jaffrey SR (2014). Broccoli: Rapid Selection of an RNA Mimic of Green Fluorescent Protein by Fluorescence-Based Selection and Directed Evolution. J. Am. Chem. Soc. 136, 16299–16308. [PubMed: 25337688]

Fleming A, Noda T, Yoshimori T, and Rubinsztein DC (2011). Chemical modulators of autophagy as biological probes and potential therapeutics. Nat Chem Biol 7, 9–17. [PubMed: 21164513]

de la Fuente-Herreruela D, Gónzalez-Charro V, Almendro-Vedia VG, Morán M, Martín MÁ, Lillo MP, Natale P, and López-Montero I. (2017). Rhodamine-based sensor for real-time imaging of mitochondrial ATP in living fibroblasts. Biochimica et Biophysica Acta (BBA) - Bioenergetics 1858, 999–1006. [PubMed: 28947254]

Galea G, and Simpson JC (2013). High-Content Screening and Analysis of the Golgi Complex. In Methods in Cell Biology, (Elsevier), pp. 281–295.

Galea G, Bexiga MG, Panarella A, O'Neill ED, and Simpson JC (2015). A high-content screening microscopy approach to dissect the role of Rab proteins in Golgi-to-ER retrograde trafficking. Journal of Cell Science 128, 2339–2349. [PubMed: 25999475]

Galganski L, Urbanek MO, and Krzyzosiak WJ (2017). Nuclear speckles: molecular organization, biological function and role in disease. Nucleic Acids Res 45, 10350–10368. [PubMed: 28977640]

Ganassi M, Mateju D, Bigi I, Mediani L, Poser I, Lee HO, Seguin SJ, Morelli FF, Vinet J, Leo G, et al. (2016). A Surveillance Function of the HSPB8-BAG3-HSP70 Chaperone Complex Ensures Stress Granule Integrity and Dynamism. Molecular Cell 63, 796–810. [PubMed: 27570075]

Giammarioli AM, Gambardella L, Barbati C, Pietraforte D, Tinari A, Alberton M, Gnessi L, Griffin RJ, Minetti M, and Malorni W. (2012). Differential effects of the glycolysis inhibitor 2-deoxy-D-glucose on the activity of pro-apoptotic agents in metastatic melanoma cells, and induction of a cytoprotective autophagic response. Int. J. Cancer 131, E337–347. [PubMed: 21913183]

Guan D, and Kao H-Y (2015). The function, regulation and therapeutic implications of the tumor suppressor protein, PML. Cell & Bioscience 5, 60. [PubMed: 26539288]

Gurrieri C, Capodieci P, Bernardi R, Scaglioni PP, Nafa K, Rush LJ, Verbel DA, Cordon-Cardo C, and Pandolfi PP (2004). Loss of the Tumor Suppressor PML in Human Cancers of Multiple Histologic Origins. J Natl Cancer Inst 96, 269–279. [PubMed: 14970276]

Gustafsson MGL, Shao L, Carlton PM, Wang CJR, Golubovskaya IN, Cande WZ, Agard DA, and Sedat JW (2008). Three-Dimensional Resolution Doubling in Wide-Field Fluorescence Microscopy by Structured Illumination. Biophysical Journal 94, 4957–4970. [PubMed: 18326650]

Gutscher M, Pauleau A-L, Marty L, Brach T, Wabnitz GH, Samstag Y, Meyer AJ, and Dick TP (2008). Real-time imaging of the intracellular glutathione redox potential. Nat Methods 5, 553–559. [PubMed: 18469822]

van Hameren G, Campbell G, Deck M, Berthelot J, Gautier B, Quintana P, Chrast R, and Tricaud N. (2019). In vivo real-time dynamics of ATP and ROS production in axonal mitochondria show decoupling in mouse models of peripheral neuropathies. Acta Neuropathologica Communications 7, 86. [PubMed: 31186069]

Hanson GT, Aggeler R, Oglesbee D, Cannon M, Capaldi RA, Tsien RY, and Remington SJ (2004). Investigating Mitochondrial Redox Potential with Redox-sensitive Green Fluorescent Protein Indicators. J. Biol. Chem. 279, 13044–13053. [PubMed: 14722062]

Harguindey S, Reshkin S, Orive G, Luis Arranz J, and Anitua E. (2007). Growth and Trophic Factors, pH and the Na+/H+ Exchanger in Alzheimers Disease, Other Neurodegenerative Diseases and Cancer: New Therapeutic Possibilities and Potential Dangers. CAR 4, 53–65.

Harwig MC, Viana MP, Egner JM, Harwig JJ, Widlansky ME, Rafelski SM, and Hill RB (2018). Methods for imaging mammalian mitochondrial morphology: A prospective on MitoGraph. Analytical Biochemistry 552, 81–99. [PubMed: 29505779]

He J-S, Soo P, Evers M, Parsons KM, Hein N, Hannan KM, Hannan RD, and George AJ (2018). High-Content Imaging Approaches to Quantitate Stress-Induced Changes in Nucleolar Morphology. ASSAY and Drug Development Technologies 16, 320–332. [PubMed: 30148664]

Hicks SW, and Machamer CE (2005). Golgi structure in stress sensing and apoptosis. Biochimica et Biophysica Acta (BBA) - Molecular Cell Research 1744, 406–414. [PubMed: 15979510]

Hirayama T, Inden M, Tsuboi H, Niwa M, Uchida Y, Naka Y, Hozumi I, and Nagasawa H. (2019). A Golgi-targeting fluorescent probe for labile Fe(ii) to reveal an abnormal cellular iron distribution induced by dysfunction of VPS35. Chem. Sci. 10, 1514–1521. [PubMed: 30809369]

Hu J, Dong L, and Outten CE (2008). The Redox Environment in the Mitochondrial Intermembrane Space Is Maintained Separately from the Cytosol and Matrix. J. Biol. Chem. 283, 29126–29134. [PubMed: 18708636]

Hussain S, Le Guezennec X, Yi W, Dong H, Chia J, Yiping K, Khoon LK, and Bard F. (2017). Digging deep into Golgi phenotypic diversity with unsupervised machine learning. MBoC 28, 3686–3698. [PubMed: 29021342]

Iannetti EF, Smeitink JAM, Beyrath J, Willems PHGM, and Koopman WJH (2016). Multiplexed high-content analysis of mitochondrial morphofunction using live-cell microscopy. Nat Protoc 11, 1693–1710. [PubMed: 27560174]

Iannetti EF, Prigione A, Smeitink JAM, Koopman WJH, Beyrath J, and Renkema H. (2019). Live-Imaging Readouts and Cell Models for Phenotypic Profiling of Mitochondrial Function. Front. Genet. 10, 131. [PubMed: 30881379]

Ilangumaran S, and Hoessli DC (1998). Effects of cholesterol depletion by cyclodextrin on the sphingolipid microdomains of the plasma membrane. Biochem J 335, 433–440. [PubMed: 9761744]

Imamura H, Huynh Nhat KP, Togawa H, Saito K, Iino R, Kato-Yamada Y, Nagai T, and Noji H. (2009). Visualization of ATP levels inside single living cells with fluorescence resonance energy transfer-based genetically encoded indicators. PNAS 106, 15651–15656. [PubMed: 19720993]

Ishida M, Watanabe H, Takigawa K, Kurishita Y, Oki C, Nakamura A, Hamachi I, and Tsukiji S. (2013). Synthetic self-localizing ligands that control the spatial location of proteins in living cells. J. Am. Chem. Soc. 135, 12684–12689. [PubMed: 23941503]

Ishii S, Matsuura A, and Itakura E. (2019). Identification of a factor controlling lysosomal homeostasis using a novel lysosomal trafficking probe. Scientific Reports 9, 11635. [PubMed: 31406169]

Jain S, Wheeler JR, Walters RW, Agrawal A, Barsic A, and Parker R. (2016). ATPase-Modulated Stress Granules Contain a Diverse Proteome and Substructure. Cell 164, 487–498. [PubMed: 26777405]

Jang J-W, Song Y, Kim KM, Kim J-S, Choi EK, Kim J, and Seo H. (2016). Hepatocellular carcinoma-targeted drug discovery through image-based phenotypic screening in co-cultures of HCC cells with hepatocytes. BMC Cancer 16, 810. [PubMed: 27756242]

Jevtic V, Kindle P, and Avilov SV (2018). SYBR Gold dye enables preferential labelling of mitochondrial nucleoids and their time-lapse imaging by structured illumination microscopy. PLoS ONE 13, e0203956.

Ji LL, Yeo D, Kang C, and Zhang T. (2020). The role of mitochondria in redox signaling of muscle homeostasis. Journal of Sport and Health Science S2095254620300089.

Joshi G, Chi Y, Huang Z, and Wang Y. (2014). Aβ-induced Golgi fragmentation in Alzheimer's disease enhances Aβ production. PNAS 111, E1230–E1239. [PubMed: 24639524]

Joshi G, Bekier MI, and Wang Y. (2015). Golgi Fragmentation in Alzheimer's Disease. Front. Neurosci. 9.

Kallunki T, Olsen OD, and Jäättelä M. (2013). Cancer-associated lysosomal changes: friends or foes? Oncogene 32, 1995–2004. [PubMed: 22777359]

Kaludercic N, Deshwal S, and Di Lisa F. (2014). Reactive oxygen species and redox compartmentalization. Front. Physiol. 5.

Kasper D, Planells-Cases R, Fuhrmann JC, Scheel O, Zeitz O, Ruether K, Schmitt A, Poët M, Steinfeld R, Schweizer M, et al. (2005). Loss of the chloride channel ClC-7 leads to lysosomal storage disease and neurodegeneration. EMBO J 24, 1079–1091. [PubMed: 15706348]

Kellokumpu S, Sormunen R, and Kellokumpu I. (2002). Abnormal glycosylation and altered Golgi structure in colorectal cancer: dependence on intra-Golgi pH. FEBS Letters 516, 217–224. [PubMed: 11959136]

Kempfer R, and Pombo A. (2020). Methods for mapping 3D chromosome architecture. Nature Reviews Genetics 21, 207–226.

Khacho M, and Slack RS (2018). Mitochondrial dynamics in the regulation of neurogenesis: From development to the adult brain. Developmental Dynamics 247, 47–53. [PubMed: 28643345]

Kimball SR, Horetsky RL, Ron D, Jefferson LS, and Harding HP (2003). Mammalian stress granules represent sites of accumulation of stalled translation initiation complexes. American Journal of Physiology-Cell Physiology 284, C273–C284. [PubMed: 12388085]

Kirkegaard T, and Jäättelä M. (2009). Lysosomal involvement in cell death and cancer. Biochimica et Biophysica Acta (BBA) - Molecular Cell Research 1793, 746–754. [PubMed: 18948147]

Koch J, Feichtinger RG, Freisinger P, Pies M, Schrödl F, Iuso A, Sperl W, Mayr JA, Prokisch H, and Haack TB (2016). Disturbed mitochondrial and peroxisomal dynamics due to loss of MFF causes Leigh-like encephalopathy, optic atrophy and peripheral neuropathy. J Med Genet 53, 270–278. [PubMed: 26783368]

Lafarga M, Tapia O, Romero AM, and Berciano MT (2016). Cajal bodies in neurons. RNA Biol 14, 712–725. [PubMed: 27627892]

Lajoie P, Fazio EN, and Snapp EL (2014). Approaches to imaging unfolded secretory protein stress in living cells. Endoplasmic Reticulum Stress Dis 1, 27–39. [PubMed: 25419521]

Lallemand-Breitenbach V, and de Thé H. (2010). PML Nuclear Bodies. Cold Spring Harb Perspect Biol 2.

Lashuel HA, and Hirling H. (2006). Rescuing Defective Vesicular Trafficking Protects against α-Synuclein Toxicity in Cellular and Animal Models of Parkinson's Disease. ACS Chem. Biol. 1, 420–424. [PubMed: 17168518]

Lee M-C, Chen Y-K, Hsu Y-J, and Lin B-R (2020). Niclosamide inhibits the cell proliferation and enhances the responsiveness of esophageal cancer cells to chemotherapeutic agents. Oncology Reports 43, 549–561. [PubMed: 31894334]

Leung AKL, Gerlich D, Miller G, Lyon C, Lam YW, Lleres D, Daigle N, Zomerdijk J, Ellenberg J, and Lamond AI (2004). Quantitative kinetic analysis of nucleolar breakdown and reassembly during mitosis in live human cells. J Cell Biol 166, 787–800. [PubMed: 15353547]

Leung K, Chakraborty K, Saminathan A, and Krishnan Y. (2019). A DNA nanomachine chemically resolves lysosomes in live cells. Nature Nanotech 14, 176–183.

Li P, Guo X, Bai X, Wang X, Ding Q, Zhang W, Zhang W, and Tang B. (2019). Golgi Apparatus Polarity Indicates Depression-Like Behaviors of Mice Using in Vivo Fluorescence Imaging. Anal. Chem. 91, 3382–3388. [PubMed: 30734552]

Li Q, Kim Y, Namm J, Kulkarni A, Rosania GR, Ahn Y-H, and Chang Y-T (2006). RNA-Selective, Live Cell Imaging Probes for Studying Nuclear Structure and Function. Chemistry & Biology 13, 615–623. [PubMed: 16793519]

Li RS, Gao PF, Zhang HZ, Zheng LL, Li CM, Wang J, Li YF, Liu F, Li N, and Huang CZ (2017). Chiral nanoprobes for targeting and long-term imaging of the Golgi apparatus. Chem. Sci. 8, 6829–6835. [PubMed: 29147508]

Li Z, Sun S, Yang Z, Zhang S, Zhang H, Hu M, Cao J, Wang J, Liu F, Song F, et al. (2013). The use of a near-infrared RNA fluorescent probe with a large Stokes shift for imaging living cells assisted by the macrocyclic molecule CB7. Biomaterials 34, 6473–6481. [PubMed: 23755836]

Liao P-C, Franco-Iborra S, Yang Y, and Pon LA (2020). Chapter 12 - Live cell imaging of mitochondrial redox state in mammalian cells and yeast. In Methods in Cell Biology, Pon LA, and Schon EA, eds. (Academic Press), pp. 295–319.

Little D, Luft C, Mosaku O, Lorvellec M, Yao Z, Paillusson S, Kriston-Vizi J, Gandhi S, Abramov AY, Ketteler R, et al. (2018). A single cell high content assay detects mitochondrial dysfunction in iPSC-derived neurons with mutations in SNCA. Sci Rep 8, 9033. [PubMed: 29899557]

Liu W, Zhou B, Niu G, Ge J, Wu J, Zhang H, Xu H, and Wang P. (2015). Deep-Red Emissive Crescent-Shaped Fluorescent Dyes: Substituent Effect on Live Cell Imaging. ACS Appl. Mater. Interfaces 7, 7421–7427. [PubMed: 25785397]

Liu Y, Jin M, Wang Y, Zhu J, Tan R, Zhao J, Ji X, Jin C, Jia Y, Ren T, et al. (2020). MCU-induced mitochondrial calcium uptake promotes mitochondrial biogenesis and colorectal cancer growth. Sig Transduct Target Ther 5, 59.

Lu Y-J, Deng Q, Hu D-P, Wang Z-Y, Huang B-H, Du Z-Y, Fang Y-X, Wong W-L, Zhang K, and Chow C-F (2015). A molecular fluorescent dye for specific staining and imaging of RNA in live cells: a novel ligand integration from classical thiazole orange and styryl compounds. Chem. Commun. 51, 15241–15244.

Lu Y-J, Deng Q, Hou J-Q, Hu D-P, Wang Z-Y, Zhang K, Luyt LG, Wong W-L, and Chow C-F (2016). Molecular Engineering of Thiazole Orange Dye: Change of Fluorescent Signaling from Universal to Specific upon Binding with Nucleic Acids in Bioassay. ACS Chem. Biol. 11, 1019–1029. [PubMed: 26752011]

Luo Y, Na Z, and Slavoff SA (2018). P-Bodies: Composition, Properties, and Functions. Biochemistry 57, 2424–2431. [PubMed: 29381060]

Maeda Y, Beznoussenko GV, Van Lint J, Mironov AA, and Malhotra V. (2001). Recruitment of protein kinase D to the trans-Golgi network via the first cysteine-rich domain. EMBO J 20, 5982–5990. [PubMed: 11689438]

Magrané J, Cortez C, Gan W-B, and Manfredi G. (2014). Abnormal mitochondrial transport and morphology are common pathological denominators in SOD1 and TDP43 ALS mouse models. Hum Mol Genet 23, 1413–1424. [PubMed: 24154542]

Major AT, Miyamoto Y, Lo CY, Jans DA, and Loveland KL (2017). Development of a pipeline for automated, high-throughput analysis of paraspeckle proteins reveals specific roles for importin α proteins. Sci Rep 7.

Markvicheva KN, Bilan DS, Mishina NM, Gorokhovatsky A.Yu, Vinokurov LM, Lukyanov S, and Belousov VV (2011). A genetically encoded sensor for H2O2 with expanded dynamic range. Bioorganic & Medicinal Chemistry 19, 1079–1084.

Marrone L, Poser I, Casci I, Japtok J, Reinhardt P, Janosch A, Andree C, Lee HO, Moebius C, Koerner E, et al. (2018). Isogenic FUS-eGFP iPSC Reporter Lines Enable Quantification of FUS Stress Granule Pathology that Is Rescued by Drugs Inducing Autophagy. Stem Cell Reports 10, 375–389. [PubMed: 29358088]

Mattson MP, Gleichmann M, and Cheng A. (2008). Mitochondria in Neuroplasticity and Neurological Disorders. Neuron 60, 748–766. [PubMed: 19081372]

McInnes J. (2013). Mitochondrial-associated metabolic disorders: foundations, pathologies and recent progress. Nutr Metab (Lond) 10, 63. [PubMed: 24499129]

Medina DL, and Ballabio A. (2015). Lysosomal calcium regulates autophagy. Autophagy 11, 970–971. [PubMed: 26000950]

Mindell JA (2012). Lysosomal acidification mechanisms. Annu. Rev. Physiol. 74, 69–86. [PubMed: 22335796]

Mitrea DM, Chandra B, Ferrolino MC, Gibbs EB, Tolbert M, White MR, and Kriwacki RW (2018). Methods for Physical Characterization of Phase-Separated Bodies and Membrane-less Organelles. Journal of Molecular Biology 430, 4773–4805. [PubMed: 30017918]

Moon SL, Morisaki T, Khong A, Lyon K, Parker R, and Stasevich TJ (2019). Multicolour single-molecule tracking of mRNA interactions with RNP granules. Nat Cell Biol 21, 162–168. [PubMed: 30664789]

Morris GE (2008). The Cajal body. Biochimica et Biophysica Acta (BBA) - Molecular Cell Research 1783, 2108–2115. [PubMed: 18755223]

Murakami T, Qamar S, Lin JQ, Schierle GSK, Rees E, Miyashita A, Costa AR, Dodd RB, Chan FTS, Michel CH, et al. (2015). ALS/FTD Mutation-Induced Phase Transition of FUS Liquid Droplets and Reversible Hydrogels into Irreversible Hydrogels Impairs RNP Granule Function. Neuron 88, 678–690. [PubMed: 26526393]

Murphy E, Ardehali H, Balaban RS, DiLisa F, Dorn GW, Kitsis RN, Otsu K, Ping P, Rizzuto R, Sack MN, et al. (2016). Mitochondrial Function, Biology, and Role in Disease: A Scientific Statement From the American Heart Association. Circ Res 118, 1960–1991. [PubMed: 27126807]

Naslavsky N, and Caplan S. (2018). The enigmatic endosome – sorting the ins and outs of endocytic trafficking. J Cell Sci 131, jcs216499.

Paige JS, Wu KY, and Jaffrey SR (2011). RNA Mimics of Green Fluorescent Protein. Science 333, 642–646. [PubMed: 21798953]

Panda PK, Fahrner A, Vats S, Seranova E, Sharma V, Chipara M, Desai P, Torresi J, Rosenstock T, Kumar D, et al. (2019). Chemical Screening Approaches Enabling Drug Discovery of Autophagy Modulators for Biomedical Applications in Human Diseases. Front. Cell Dev. Biol. 7, 38. [PubMed: 30949479]

Paroutis P, Touret N, and Grinstein S. (2004). The pH of the Secretory Pathway: Measurement, Determinants, and Regulation. Physiology 19, 207–215. [PubMed: 15304635]

Pederson T. (2011). The Nucleolus. Cold Spring Harb Perspect Biol 3, a000638.

Peng Y, Gao P, Shi L, Chen L, Liu J, and Long J. (2020). Central and Peripheral Metabolic Defects Contribute to the Pathogenesis of Alzheimer's Disease: Targeting Mitochondria for Diagnosis and Prevention. Antioxidants & Redox Signaling 32, 1188–1236. [PubMed: 32050773]

Perrin DD (1965). Dissociation constants of organic bases in aqueous solution (London: Butterworths).

Petrosyan A. (2015). Onco-Golgi: Is Fragmentation a Gate to Cancer Progression? Biochem Mol Biol J 1.

Piattoni CV, Sardi F, Klein F, Pantano S, Bollati-Fogolin M, and Comini M. (2019). New red-shifted fluorescent biosensor for monitoring intracellular redox changes. Free Radical Biology and Medicine 134, 545–554. [PubMed: 30735840]

Platani M, Goldberg I, Swedlow JR, and Lamond AI (2000). In Vivo Analysis of Cajal Body Movement, Separation, and Joining in Live Human Cells. J Cell Biol 151, 1561–1574. [PubMed: 11134083]

Pohan G, Espinosa JA, Chen S, Ang KK, Arkin MR, and Markossian S. (2020). Multiparametric High-Content Assays to Measure Cell Health and Oxidative Damage as a Model for Drug-Induced Liver Injury. Current Protocols in Chemical Biology 12, e90.

Policarpio-Nicolas MLC, and Sirohi D. (2013). Macrofollicular variant of papillary carcinoma, a potential diagnostic pitfall: A report of two cases including a review of literature. Cytojournal 10.

Ponsford AH, Ryan TA, Raimondi A, Cocucci E, Wycislo SA, Fröhlich F, Swan LE, and Stagi M. (2020). Live imaging of intra-lysosome pH in cell lines and primary neuronal culture using a novel genetically encoded biosensor. Autophagy 1–19.

Pugach EK, Feltes M, Kaufman RJ, Ory DS, and Bang AG (2018). High-content screen for modifiers of Niemann-Pick type C disease in patient cells. Hum Mol Genet 27, 2101–2112. [PubMed: 29659804]

Reineke EL, and Kao H-Y (2009). PML: An emerging tumor suppressor and a target with therapeutic potential. Cancer Ther 7, 219–226. [PubMed: 19756257]

Rivinoja A, Pujol FM, Hassinen A, and Kellokumpu S. (2012). Golgi pH, its regulation and roles in human disease. Annals of Medicine 44, 542–554. [PubMed: 21585247]

Rosania GR, Lee JW, Ding L, Yoon H-S, and Chang Y-T (2003). Combinatorial Approach to Organelle-Targeted Fluorescent Library Based on the Styryl Scaffold. J. Am. Chem. Soc. 125, 1130–1131. [PubMed: 12553790]

Rosenbaum AI, Zhang G, Warren JD, and Maxfield FR (2010). Endocytosis of beta-cyclodextrins is responsible for cholesterol reduction in Niemann-Pick type C mutant cells. Proc Natl Acad Sci U S A 107, 5477–5482. [PubMed: 20212119]

Ryu H-H, Jun M-H, Min K-J, Jang D-J, Lee Y-S, Kim HK, and Lee J-A (2014). Autophagy regulates amyotrophic lateral sclerosis-linked fused in sarcoma-positive stress granules in neurons. Neurobiology of Aging 35, 2822–2831. [PubMed: 25216585]

Saha S, Prakash V, Halder S, Chakraborty K, and Krishnan Y. (2015). A pH-independent DNA nanodevice for quantifying chloride transport in organelles of living cells. Nature Nanotechnology 10, 645–651.

Scott I, and Youle RJ (2010). Mitochondrial fission and fusion. Essays Biochem 47, 85–98. [PubMed: 20533902]

Scotto Rosato A, Montefusco S, Soldati C, Di Paola S, Capuozzo A, Monfregola J, Polishchuk E, Amabile A, Grimm C, Lombardo A, et al. (2019). TRPML1 links lysosomal calcium to autophagosome biogenesis through the activation of the CaMKKβ/VPS34 pathway. Nat Commun 10.

Settembre C, Fraldi A, Medina DL, and Ballabio A. (2013). Signals for the lysosome: a control center for cellular clearance and energy metabolism. Nat Rev Mol Cell Biol 14, 283–296. [PubMed: 23609508]

Shlevkov E, Basu H, Bray M-A, Sun Z, Wei W, Apaydin K, Karhohs K, Chen P-F, Smith JLM, Wiskow O, et al. (2019). A High-Content Screen Identifies TPP1 and Aurora B as Regulators of Axonal Mitochondrial Transport. Cell Reports 28, 3224–3237.e5.

Shorter J, Beard MB, Seemann J, Dirac-Svejstrup AB, and Warren G. (2002). Sequential tethering of Golgins and catalysis of SNAREpin assembly by the vesicle-tethering protein p115. J Cell Biol 157, 45–62. [PubMed: 11927603]

Shu C-W, Liu P-F, and Huang C-M (2012). High Throughput Screening for Drug Discovery of Autophagy Modulators. CCHTS 15, 721–729.

Song G, Sun Y, Liu Y, Wang X, Chen M, Miao F, Zhang W, Yu X, and Jin J. (2014). Low molecular weight fluorescent probes with good photostability for imaging RNA-rich nucleolus and RNA in cytoplasm in living cells. Biomaterials 35, 2103–2112. [PubMed: 24332461]

Soo KY, Halloran M, Sundaramoorthy V, Parakh S, Toth RP, Southam KA, McLean CA, Lock P, King A, Farg MA, et al. (2015). Rab1-dependent ER–Golgi transport dysfunction is a common pathogenic mechanism in SOD1, TDP-43 and FUS-associated ALS. Acta Neuropathol 130, 679–697. [PubMed: 26298469]

Spang A. (2013). Retrograde Traffic from the Golgi to the Endoplasmic Reticulum. Cold Spring Harb Perspect Biol 5, a013391.

Spector DL, and Lamond AI (2011). Nuclear Speckles. Cold Spring Harb Perspect Biol 3.

Steffan JJ, Snider JL, Skalli O, Welbourne T, and Cardelli JA (2009). Na+/H+ Exchangers and RhoA Regulate Acidic Extracellular pH-Induced Lysosome Trafficking in Prostate Cancer Cells. Traffic 10, 737–753. [PubMed: 19302267]

Steffan JJ, Coleman DT, and Cardelli JA (2011). The HGF-met signaling axis: emerging themes and targets of inhibition. Curr. Protein Pept. Sci. 12, 12–22. [PubMed: 21190524]

Stoka V, Turk V, and Turk B. (2016). Lysosomal cathepsins and their regulation in aging and neurodegeneration. Ageing Research Reviews 32, 22–37. [PubMed: 27125852]

Thompson AD, Bewersdorf J, Toomre D, and Schepartz A. (2017). HIDE Probes: A New Toolkit for Visualizing Organelle Dynamics, Longer and at Super-Resolution. Biochemistry 56, 5194–5201. [PubMed: 28792749]

To T-L, Piggott BJ, Makhijani K, Yu D, Jan YN, and Shu X. (2015). Rationally designed fluorogenic protease reporter visualizes spatiotemporal dynamics of apoptosis in vivo. Proc Natl Acad Sci USA 112, 3338–3343. [PubMed: 25733847]

Tomas A, Futter CE, and Eden ER (2014). EGF receptor trafficking: consequences for signaling and cancer. Trends Cell Biol 24, 26–34. [PubMed: 24295852]

Tommasino C, Gambardella L, Buoncervello M, Griffin RJ, Golding BT, Alberton M, Macchia D, Spada M, Cerbelli B, d'Amati G, et al. (2016). New derivatives of the antimalarial drug Pyrimethamine in the control of melanoma tumor growth: an in vitro and in vivo study. J Exp Clin Cancer Res 35.

Tomsic J, He H, Akagi K, Liyanarachchi S, Pan Q, Bertani B, Nagy R, Symer DE, Blencowe BJ, and Chapelle A. de la (2015). A germline mutation in SRRM2, a splicing factor gene, is implicated in papillary thyroid carcinoma predisposition. Scientific Reports 5, 10566. [PubMed: 26135620]

Tripathi V, Song DY, Zong X, Shevtsov SP, Hearn S, Fu X-D, Dundr M, and Prasanth KV (2012). SRSF1 regulates the assembly of pre-mRNA processing factors in nuclear speckles. Mol Biol Cell 23, 3694–3706. [PubMed: 22855529]

Tuma RS, Beaudet MP, Jin X, Jones LJ, Cheung C-Y, Yue S, and Singer VL (1999). Characterization of SYBR Gold Nucleic Acid Gel Stain: A Dye Optimized for Use with 300-nm Ultraviolet Transilluminators. Analytical Biochemistry 268, 278–288. [PubMed: 10075818]

Valm AM, Cohen S, Legant WR, Melunis J, Hershberg U, Wait E, Cohen AR, Davidson MW, Betzig E, and Lippincott-Schwartz J. (2017). Applying systems-level spectral imaging and analysis to reveal the organelle interactome. Nature 546, 162–167. [PubMed: 28538724]

Varkuti BH, Liu Z, Kepiro M, Pacifico R, Gai Y, Kamenecka T, and Davis RL (2020). High-Throughput Small Molecule Screen Identifies Modulators of Mitochondrial Function in Neurons. IScience 23, 100931.

Vila MC, Rayavarapu S, Hogarth MW, Van der Meulen JH, Horn A, Defour A, Takeda S, Brown KJ, Hathout Y, Nagaraju K, et al. (2017). Mitochondria mediate cell membrane repair and contribute to Duchenne muscular dystrophy. Cell Death & Differentiation 24, 330–342. [PubMed: 27834955]

Vringer E, and Tait SWG (2019). Mitochondria and Inflammation: Cell Death Heats Up. Front. Cell Dev. Biol. 7, 100. [PubMed: 31316979]

Wang C, Lu T, Emanuel G, Babcock HP, and Zhuang X. (2019). Imaging-based pooled CRISPR screening reveals regulators of lncRNA localization. PNAS 116, 10842–10851. [PubMed: 31085639]

Wang L-H, Xu M, Fu L-Q, Chen X-Y, and Yang F. (2018). The Antihelminthic Niclosamide Inhibits Cancer Stemness, Extracellular Matrix Remodeling, and Metastasis through Dysregulation of the Nuclear β-catenin/c-Myc axis in OSCC. Scientific Reports 8, 12776. [PubMed: 30143678]

Wang W, Li L, Lin W-L, Dickson DW, Petrucelli L, Zhang T, and Wang X. (2013). The ALS disease-associated mutant TDP-43 impairs mitochondrial dynamics and function in motor neurons. Hum Mol Genet 22, 4706–4719. [PubMed: 23827948]

Waris S, Wilce MCJ, and Wilce JA (2014). RNA Recognition and Stress Granule Formation by TIA Proteins. Int J Mol Sci 15, 23377–23388. [PubMed: 25522169]

Waterham HR, Koster J, van Roermund CWT, Mooyer PAW, Wanders RJA, and Leonard JV (2007). A Lethal Defect of Mitochondrial and Peroxisomal Fission. N Engl J Med 356, 1736–1741. [PubMed: 17460227]

Webb BA, Aloisio FM, Charafeddine RA, Cook J, Wittmann T, & Barber DL (2020). pHLARE: A New Biosensor Reveals Decreased Lysosome pH in Cancer Cells. Molecular Biology of the Cell, mbc.E20–06-0383.

Weber SC, and Brangwynne CP (2012). Getting RNA and Protein in Phase. Cell 149, 1188–1191. [PubMed: 22682242]

Weinert S, Jabs S, Supanchart C, Schweizer M, Gimber N, Richter M, Rademann J, Stauber T, Kornak U, and Jentsch TJ (2010). Lysosomal pathology and osteopetrosis upon loss of H+-driven lysosomal Cl- accumulation. Science 328, 1401–1403. [PubMed: 20430974]

Weiss LE, Naor T, and Shechtman Y. (2018). Observing DNA in live cells. Biochem Soc Trans 46, 729–740. [PubMed: 29871877]

Werley CA, Boccardo S, Rigamonti A, Hansson EM, and Cohen AE (2020). Multiplexed Optical Sensors in Arrayed Islands of Cells for multimodal recordings of cellular physiology. Nat Commun 11, 3881. [PubMed: 32753572]

Wolfe DM, Lee J, Kumar A, Lee S, Orenstein SJ, and Nixon RA (2013). Autophagy failure in Alzheimer's disease and the role of defective lysosomal acidification. Eur J Neurosci 37, 1949–1961. [PubMed: 23773064]

Wolozin B, and Ivanov P. (2019). Stress granules and neurodegeneration. Nat Rev Neurosci 20, 649–666. [PubMed: 31582840]

Xu D, Joglekar AP, Williams AL, and Hay JC (2000). Subunit Structure of a Mammalian ER/Golgi SNARE Complex. J. Biol. Chem. 275, 39631–39639. [PubMed: 11035026]

Xu M, Liu K, Swaroop M, Sun W, Dehdashti SJ, McKew JC, and Zheng W. (2014). A Phenotypic Compound Screening Assay for Lysosomal Storage Diseases. J Biomol Screen 19, 168–175. [PubMed: 23983233]

Yatsuzuka K, Sato S, Pe KB, Katsuda Y, Takashima I, Watanabe M, and Uesugi M. (2018). Live-cell imaging of multiple endogenous mRNAs permits the direct observation of RNA granule dynamics. Chem. Commun. 54, 7151–7154.

Yip KW, Cuddy M, Pinilla C, Giulanotti M, Heynen-Genel S, Matsuzawa S, and Reed JC (2011). A High Content Screening (HCS) Assay for the Identification of Chemical Inducers of PML Oncogenic Domains (PODs). J Biomol Screen 16, 251–258. [PubMed: 21233309]

Yue Y, Huo F, Lee S, Yin C, and Yoon J. (2016). A review: the trend of progress about pH probes in cell application in recent years. Analyst 142, 30–41. [PubMed: 27757447]

Zhang B, Wang D, Guo F, and Xuan C. (2015). Mitochondrial membrane potential and reactive oxygen species in cancer stem cells. Familial Cancer 14, 19–23. [PubMed: 25266577]

Zhang R, Niu G, Li X, Guo L, Zhang H, Yang R, Chen Y, Yu X, and Tang BZ (2019). Reaction-free and MMP-independent fluorescent probes for long-term mitochondria visualization and tracking. Chem. Sci. 10, 1994–2000. [PubMed: 30881628]

Zhang T, Mishra P, Hay BA, Chan D, and Guo M. (2017). Valosin-containing protein (VCP/p97) inhibitors relieve Mitofusin-dependent mitochondrial defects due to VCP disease mutants. ELife 6.

Zhou B, Liu W, Zhang H, Wu J, Liu S, Xu H, and Wang P. (2015). Imaging of nucleolar RNA in living cells using a highly photostable deep-red fluorescent probe. Biosensors and Bioelectronics 68, 189–196. [PubMed: 25569876]

Zhu H, Fan J, Du J, and Peng X. (2016). Fluorescent Probes for Sensing and Imaging within Specific Cellular Organelles. Acc. Chem. Res. 49, 2115–2126. [PubMed: 27661761]

HIGHLIGHTS

- Organelle structure and function can be probed for phenotypic drug screening
- Mitochondria, lysosomes, Golgi, and MLOs are active areas of probe development
- Emergent probes improve subcellular targeting and measure organelle functions

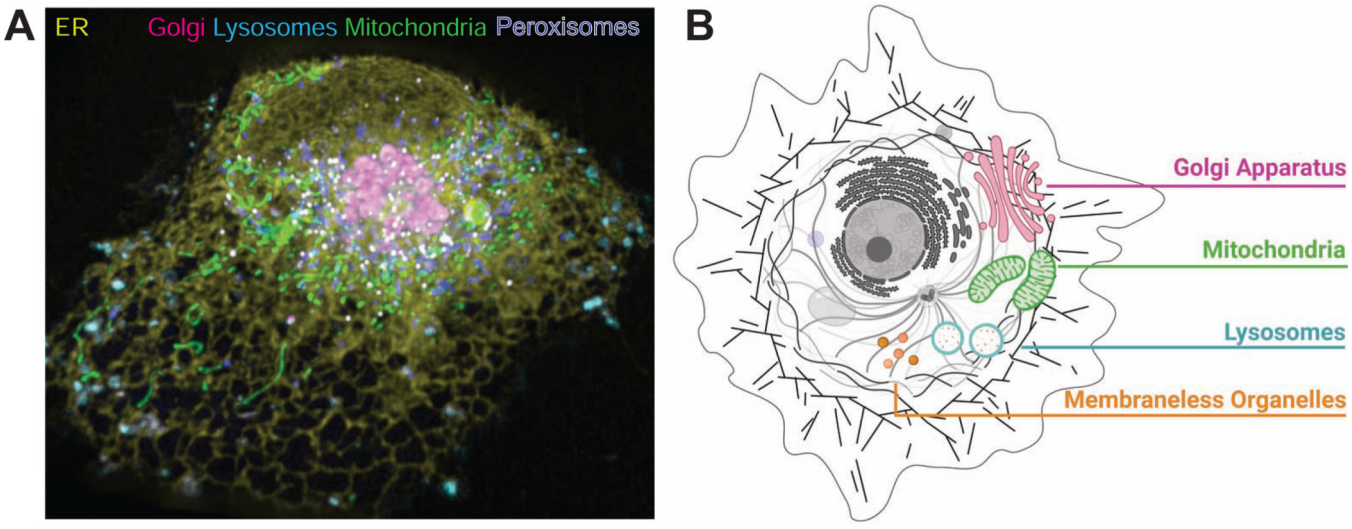

Figure 1. Organelle-specific probes elucidate intricate networks and a multitude of foci within the animal cell.

(A) Maximum intensity projection of images captured by a multispectral lattice light sheet microscope of a COS-7 cell either expressing fluorescent proteins or labeled with dyes targeting different organelles including the endoplasmic reticulum (ER), lipid droplets (LDs), the Golgi, lysosomes, mitochondria, and peroxisomes (adapted with permission from Cohen et al., 2018). (B) A schematic depicting the major organelles in an animal cell and highlighting the organelles that are the focus of this review. See also Table S1. Created with BioRender.com.

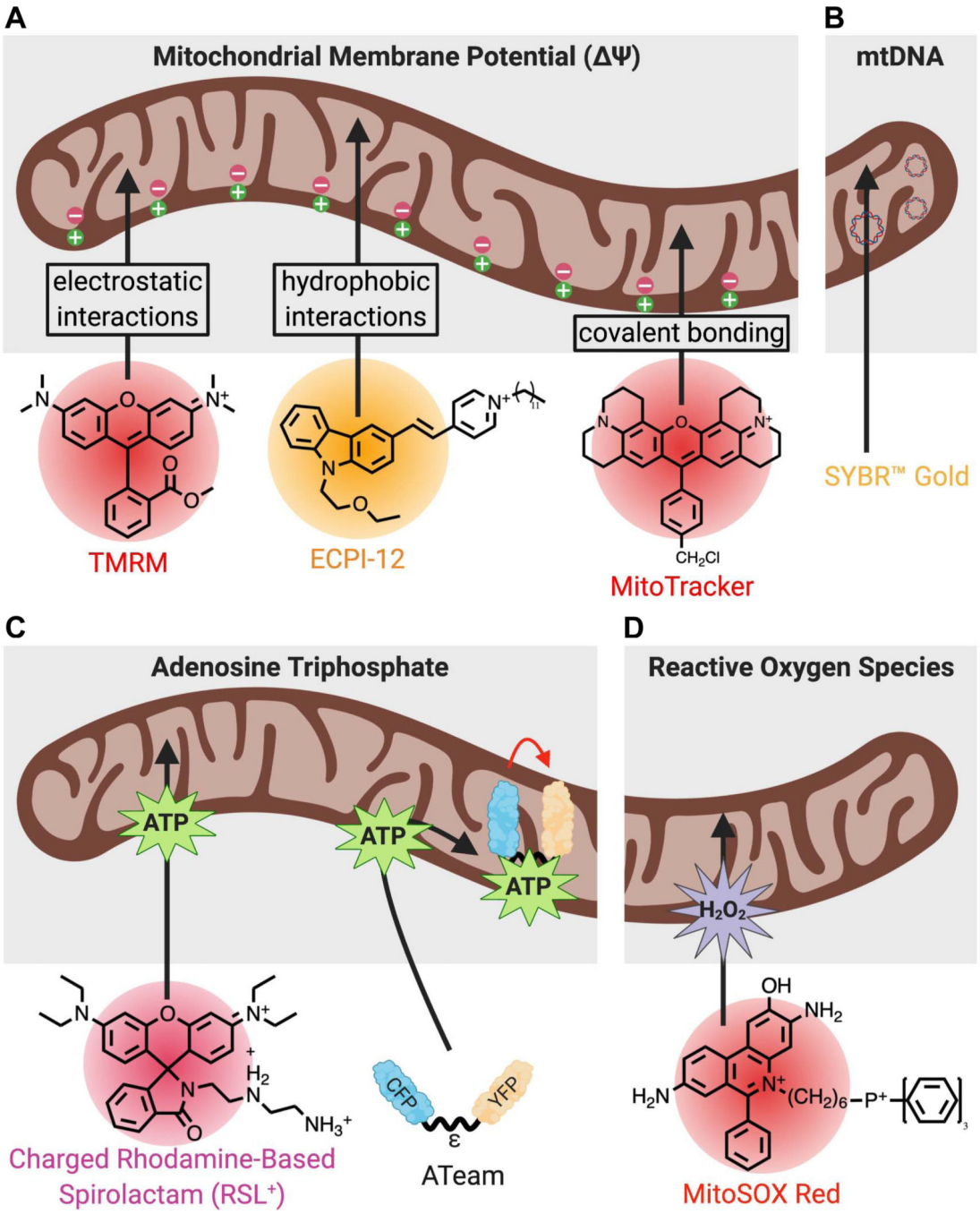

Figure 2. Examples of biomarkers used in live-cell readouts to quantify mitochondrial health.

(A) Cationic fluorophores that target the negative mitochondrial membrane potential (ΔΨ) in the matrix. Tetramethylrhodamine methyl ester (TMRM) is a functional probe that uses electrostatic interactions with the polarized ΔΨ to directly measure changes in ΔΨ (Elmore et al., 2004). (*E*)-1-dodecyl-4-(2-(9-(2-ethoxyethyl)-9*H*-carbazol-3-yl)vinyl)pyridin-1-ium iodide (ECPI-12) is a structural probe that uses reaction-free lipophilic interactions with the mitochondrial inner membrane (Zhang et al., 2019). MitoTrackers are structural probes that irreversibly bind to thiol groups to permanently stain mitochondria independent of ΔΨ

fluctuations (Chazotte, 2011). (B) The proprietary mitochondrial DNA (mtDNA) probe SYBR Gold binds directly to mtDNA present in mitochondrial nucleoids (Jevtic et al., 2018). (C) Probes designed to target ATP include charged rhodamine-based spirolactams (RSL^+) and Adenosine 5-Triphosphate indicator based on Epsilon subunit for Analytical Measurements (ATeam) (Imamura et al., 2009). ATeam is shown with the epsilon (ε) subunit flanked between Cyan Fluorescent Protein (CFP) and Yellow Fluorescent Protein (YFP). (D) MitoSOX Red targets reactive oxygen species (ROS) within live mitochondria (De Biasi et al., 2016). Created with BioRender.com.

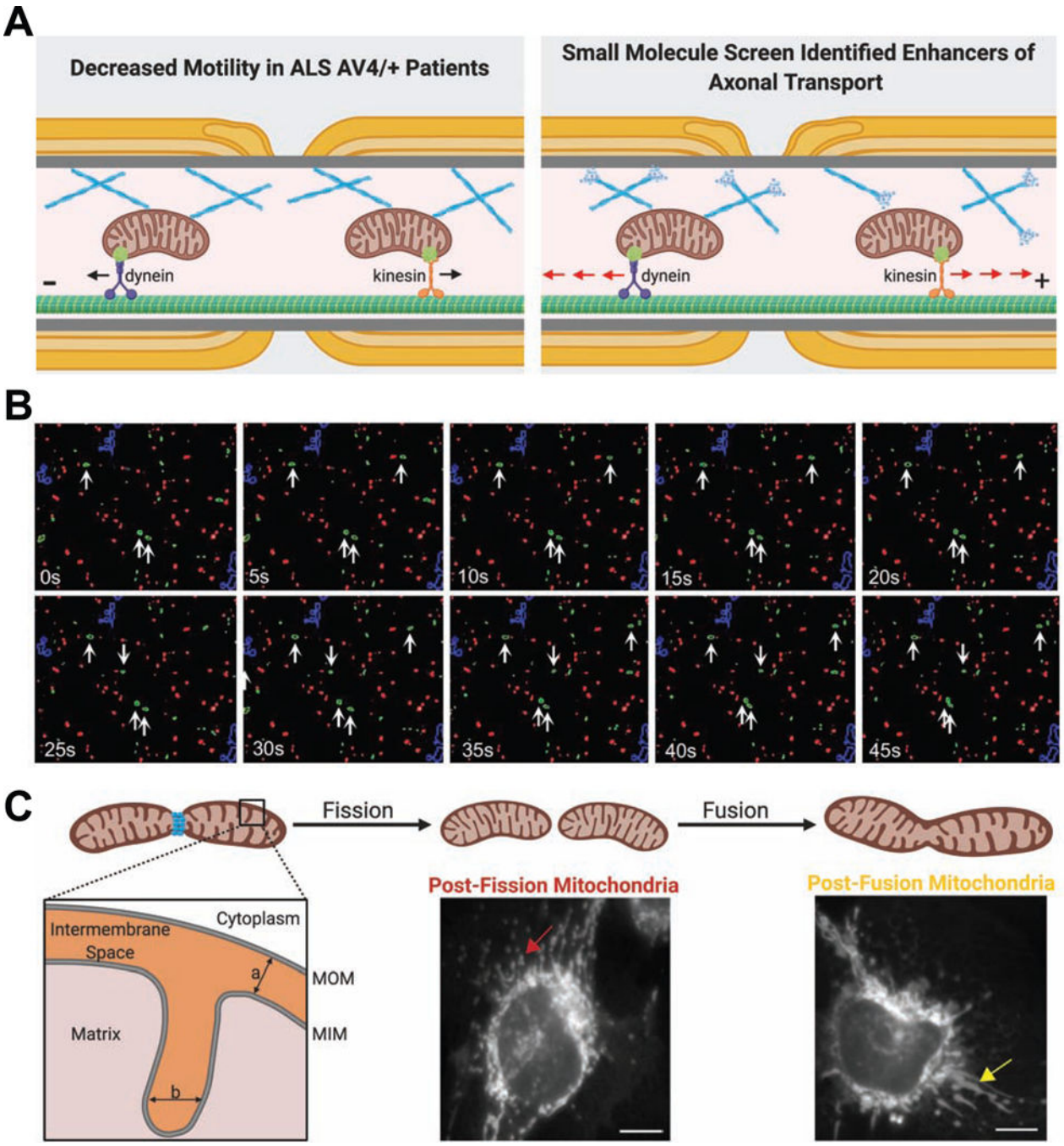

Figure 3. Examples of mitochondrial phenotypes amenable to HCA and HTS studies.

(A) High-throughput screening identified aurora kinase B (AurKB), tripeptidyl peptidase 1 (TPP1), and F-actin as targets of mitochondrial axonal trafficking in iPSC-derived neurons from an ALS patient (Shlevkov et al., 2019). (B) Minimum intensity projection of a time-lapse sequence showing stationary (red) versus motile (green) mitochondria. White arrows indicate objects that exhibit significant movement. Images were adapted from (Shlevkov et al., 2019) with permission. (C) Schematic of mitochondrial morphofunction. Structural parameters shown are mitochondrial outer membrane (MOM), mitochondrial inner

membrane (MIM), distance between MOM and MIM (labeled “a”) and intercristae space (labeled “b”) (Bulthuis et al., 2019). Live imaging of mitochondrial morphology using MitoTracker probes show fragmented mitochondria (post-fission; red arrow) and elongated mitochondria (post fusion; yellow arrow). Scale bar represents 10 μm. Microscopy images were adapted from (Harwig et al., 2018) with permission. Created with BioRender.com.

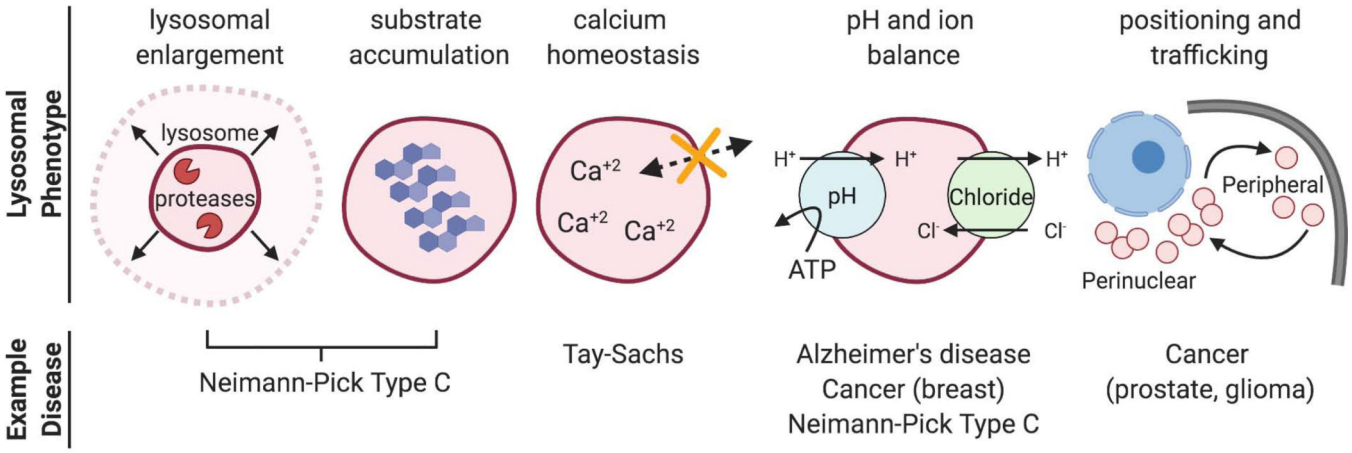

Figure 4. Lysosomal phenotypes and diseases highlighted in recently developed probes and HTS studies.

References (from left to right): Lysosomal enlargement (Xu et al., 2014); substrate accumulation (Pugach et al., 2018); calcium homeostasis (Colussi et al., 2019); pH and ion balance (Chen et al., 2015; Leung et al., 2019; Chin et al., 2020; Ponsford et al., 2020; Webb et al., 2020); Positioning and trafficking (Circu et al., 2016; Ishii et al., 2019). Created with BioRender.com.

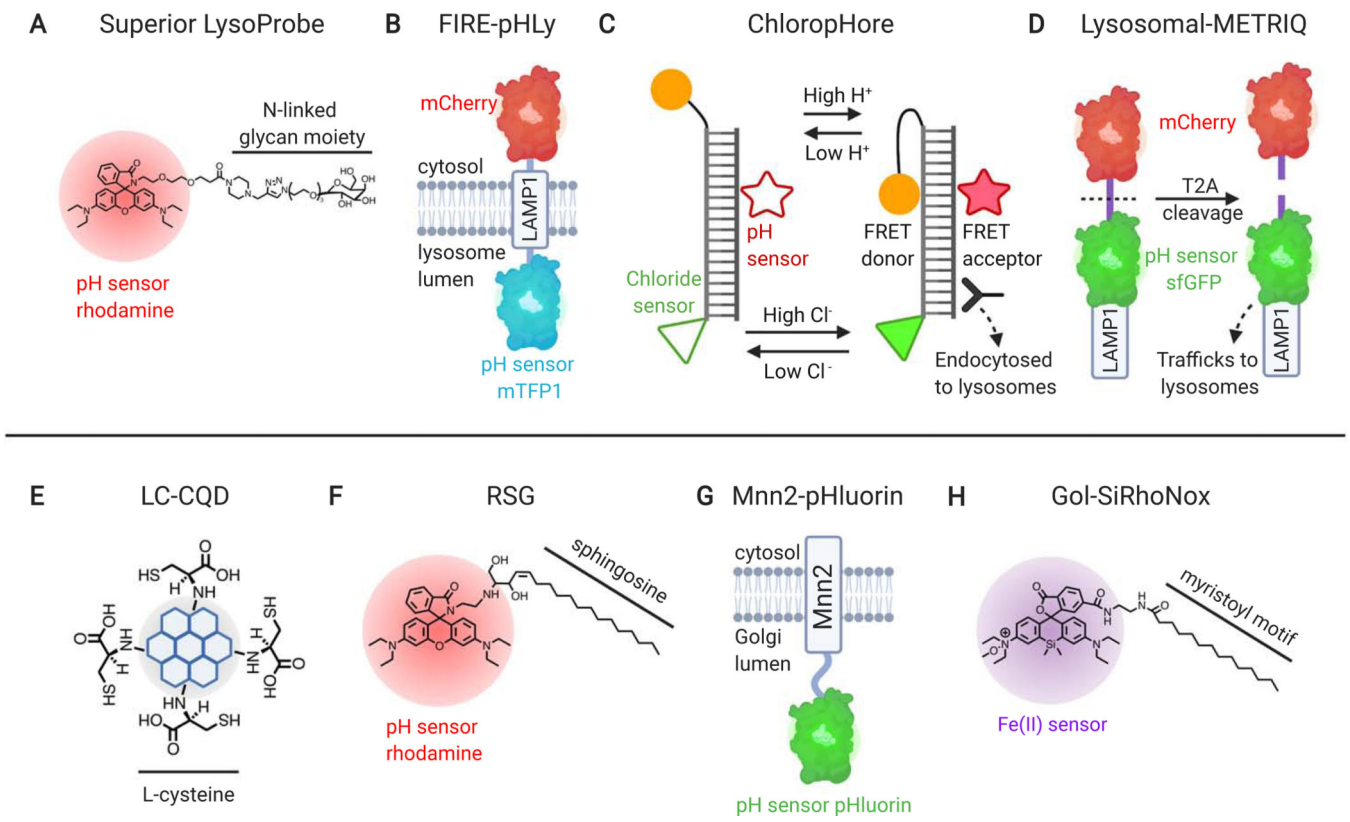

Figure 5. Examples of lysosome- and Golgi-targeted probes.

(A) Superior LysoProbe, pH-sensitive rhodamine conjugated with N-linked glycan moieties for improved lysosomal targeting; Chen et al., 2015. (B) FIRE-pHLy, ratiometric pH sensor chimera with cyan fluorescent protein, mTFP1, and LAMP1 for targeting; Chin et al., 2020. (C) ChloropHore, DNA-based dual-ion reporter for lysosomal pH (FRET-induced) and intraluminal chloride; Leung et al., 2019. (D) Lysosomal-METRIQ, self-cleaving ratiometric probe for membrane trafficking and lysosomal integrity; Ishii et al., 2019. (E) L-cysteine carbon quantum dots (LC-CQD) with functionalized cysteines for Golgi anchoring; R. S. Li et al., 2017. (F) Rhodamine-sphingosine (RSG), pH sensor conjugated with lipid sphingosine for Golgi recognition; Fan et al., 2019. (G) Mnn2-pHluorin, green fluorescent protein pH sensor targeted to Golgi membranes; Deschamps et al., 2020. (H) Gol-SiRhoNox, Fe(II) sensor with myristoyl motif for Golgi targeting; Hirayama et al., 2019. Created with BioRender.com.

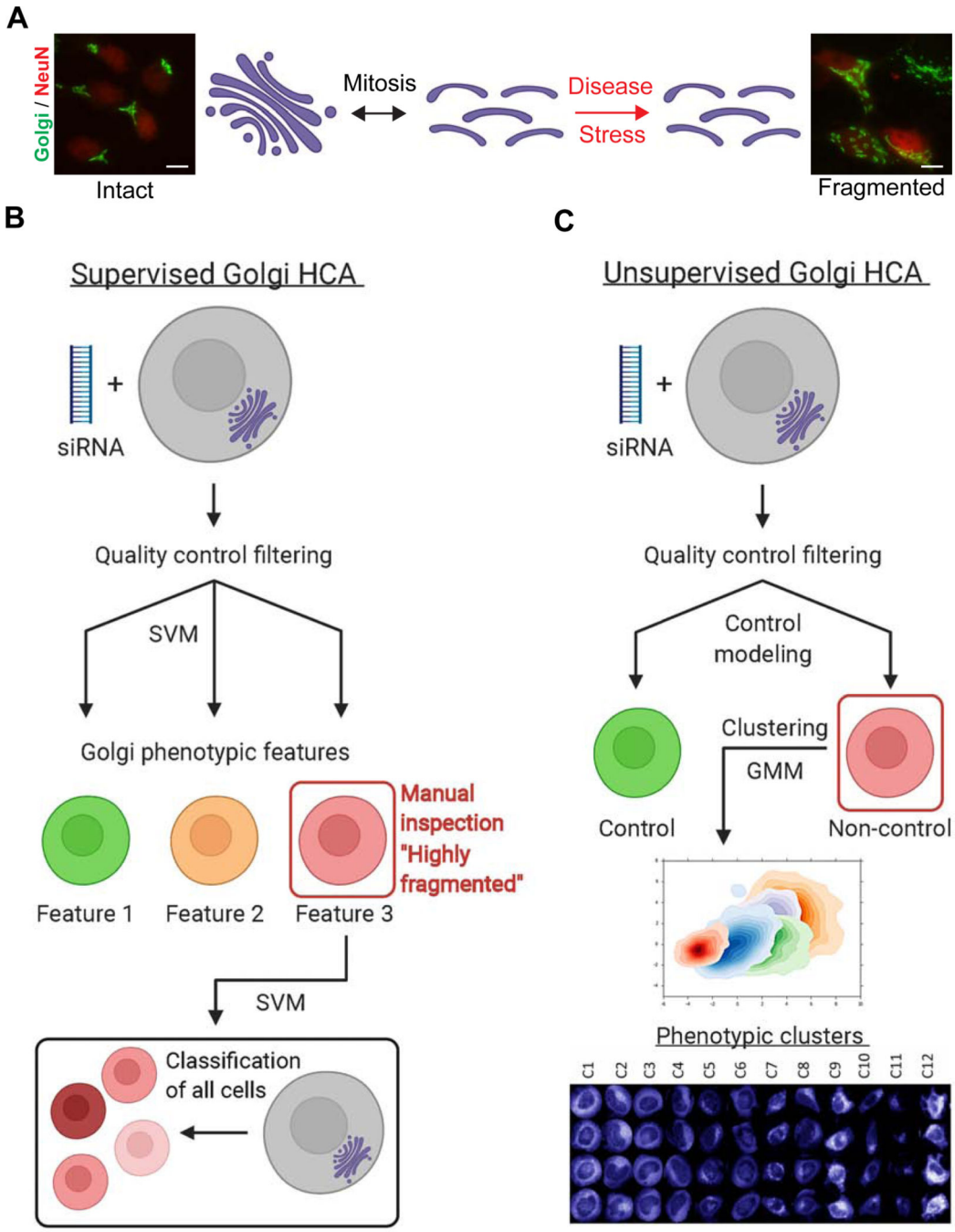

Figure 6. Golgi morphological states and HCA quantification methodologies.

(A) Schematic of Golgi structural dynamics during mitosis and disease or stress conditions. Images show representative intact and fragmented Golgi phenotypes (courtesy of Dr. Yanzhuang Wang, University of Michigan). Primary hippocampal neurons were treated with control or amyloid-beta peptides and stained for Golgi reassembly-stacking protein of 65 kDa, GRASP65 (green) and neuron marker, NeuN (red). Scale bars in all images, 10 μm. (B) Example of supervised Golgi HCA workflow (Galea and Simpson, 2013). Reference samples were chosen to manually pre-define Golgi phenotypes. Single vector machine

(SVM), one type of machine learning algorithm, then developed a classification model based on whichever features distinguished the phenotypes from each other. The resulting model was then applied to new samples to quantify the presence of these phenotypes. (C) Example of unsupervised method to classify and cluster Golgi fragmentation phenotypes in siRNA gene knockdown cells (Hussain et al., 2017). Machine learning was applied on mock control cells to separate control-like and non-control-like states without pre-specifying phenotypes. Non-control-like phenotypes were then clustered according to a Gaussian mixture model (GMM), a probabilistic model that learns the differences between normally distributed but potentially overlapping subpopulations, i.e. one specific Golgi phenotype, within an overall population, i.e. all Golgi phenotypes. Created with BioRender.com.

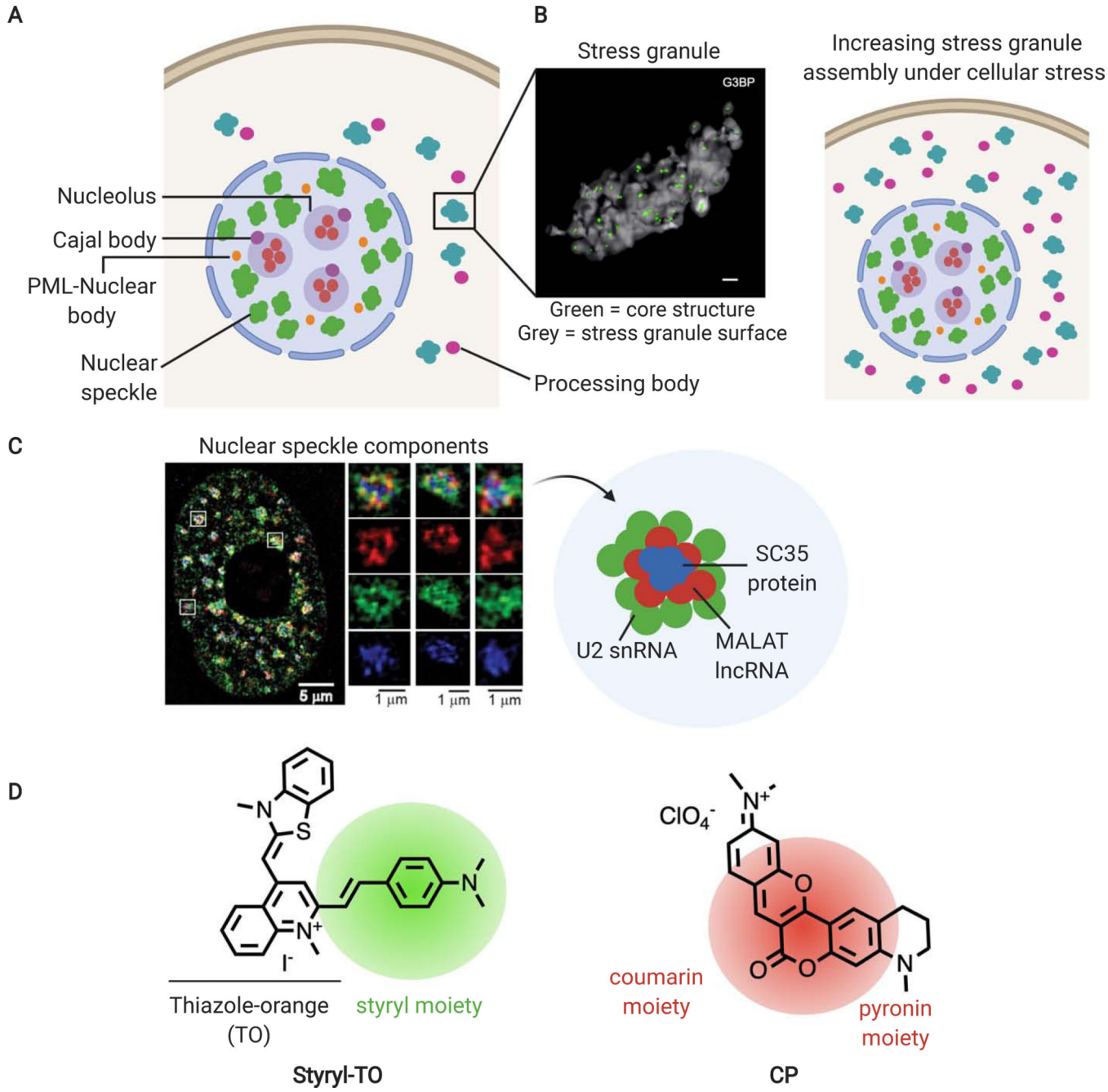

Figure 7. Membraneless organelle (MLO) localization, function, and organization examples.

(A) Schematic diagram of MLOs. (B) Three-dimensional stochastic optical reconstruction microscopy (STORM) of stress granule (SG) with green dots showing the area with high G3BP protein concentration (core) and grey surface showing area with less concentrated material (granule shell), scale bar: 500 nm. SG assembly increases in response to cellular stress. (C) Structured illumination microscopy (SIM) of nuclear speckle components. Three speckles confined in white squares were enlarged for better visualization, revealing spatial organization of U2 snRNAs, MALAT long noncoding RNAs (lncRNAs), and SC35 proteins. STORM and SIM images were adapted from (Jain et al., 2016) and (Fei et al., 2017),

respectively, with permissions. (D) Example of small molecule probes for nucleoli rDNA detection: A thiazole orange (TO)-based dye with a styryl substituent (Styryl-TO), and for rRNA detection: hybridized coumarin and pyronin moieties (CP) (Liu et al., 2015; Lu et al., 2016). Colors represent dyes' emission wavelengths. See also Table S2. Created with BioRender.com.